






Article

Trace Element Patterns in Shells of Mussels (Bivalvia) Allow to Distinguish between Fresh- and Brackish-Water Coastal Environments of the Subarctic and Boreal Zone

Artem A. Lyubas ¹, Irina A. Kuznetsova ¹, Galina V. Bovykina ¹ , Tatyana A. Eliseeva ¹, Mikhail Yu. Gofarov ¹, Irina S. Khrebtova ¹, Alexander V. Kondakov ¹ , Alexey V. Malkov ², Vasileios Mavromatis ³, Alexander R. Shevchenko ¹, Alena A. Soboleva ¹ , Oleg S. Pokrovsky ^{4,5}  and Ivan N. Bolotov ^{1,*} 

¹ N. Laverov Federal Center for Integrated Arctic Research of the Ural Branch of the Russian Academy of Sciences, Nikolsky Prospect 20, 163020 Arkhangelsk, Russia; lyubas@ro.ru (A.A.L.); akondakov@yandex.ru (A.V.K.); tomilova_aliona@mail.ru (A.A.S.)

² Scientific Department, Northern (Arctic) Federal University, Northern Dvina Emb. 17, 163000 Arkhangelsk, Russia

³ Institute of Geological Sciences, University of Bern, Baltzerstrasse 1+3, 3012 Bern, Switzerland

⁴ Geosciences and Environment Toulouse, UMR 5563 CNRS, 31400 Toulouse, France

⁵ BIO-GEO-CLIM Laboratory, Tomsk State University, 634050 Tomsk, Russia

* Correspondence: inepras@yandex.ru

Abstract: The accumulation of trace metals in the shells of bivalves allows quantitative assessments of environmental pollution and helps to reconstruct paleo aquatic environments. However, the understanding on how marine and freshwater mollusks control the level of trace elements in their shells remains very limited. Here, we compared the trace element composition of marine and freshwater bivalves from boreal and subarctic habitats, using examples of widely distributed species of marine (*Mytilus edulis*, *M. trossulus*) and freshwater (*Anodonta anatina*, *Unio* sp., *Beringiana beringiana*) mussels. Sizable differences in several trace element concentrations were detected between different species, depending on their environmental niches. A multiparametric statistical treatment of the shell's elemental composition allowed to distinguish the impact of external factors (water and sediment chemical composition) from active metabolic (biological) control. In particular, the obtained results demonstrated that Ba:Ca and Pb:Ca ratios in mussels' shells are closely related to the primary productivity of aquatic ecosystems. The Mn:Ca ratio allowed to constrain the environmental conditions of mussels' species depending on the trophic state of inhabited waterbody. Overall, the marine mussels exhibited stronger biological control of trace element accumulation, whereas trace element pattern in shells of freshwater mussels was chiefly controlled by environmental factors. The obtained results might help to use the trace element composition of bivalves in distinguishing marine and freshwater habitats of mollusks in paleo environments.

Keywords: mussels; trace element; water; sediment; coastal ecosystems; rivers; boreal; subarctic



Citation: Lyubas, A.A.; Kuznetsova, I.A.; Bovykina, G.V.; Eliseeva, T.A.; Gofarov, M.Y.; Khrebtova, I.S.; Kondakov, A.V.; Malkov, A.V.; Mavromatis, V.; Shevchenko, A.R.; et al. Trace Element Patterns in Shells of Mussels (Bivalvia) Allow to Distinguish between Fresh- and Brackish-Water Coastal Environments of the Subarctic and Boreal Zone. *Water* **2023**, *15*, 3625. <https://doi.org/10.3390/w15203625>

Academic Editor: Ryszard Gołdyn

Received: 10 September 2023

Revised: 5 October 2023

Accepted: 12 October 2023

Published: 16 October 2023



Copyright: © 2023 by the authors. Licensee MDPI, Basel, Switzerland. This article is an open access article distributed under the terms and conditions of the Creative Commons Attribution (CC BY) license (<https://creativecommons.org/licenses/by/4.0/>).

1. Introduction

Elemental composition of bivalve shells provides useful information on seasonal, annual, and historical variations in water chemical composition. Some marine and freshwater bivalve mollusks may allow to reconstruct such processes on scales up to hundreds of years, as it was shown for the long-lived marine bivalve *Arctica islandica* [1] and for freshwater pearl mussels from the genus *Margaritifera* [2–4]. Using several geochemical indicators, these authors demonstrated that climate fluctuations could be approximated by Mn:Ca, Ba:Ca, Sr:Ca ratios, and others, which helps to assess environmental changes in waterbodies.

Several indicators were successfully applied for characterizing molluscan ecology and investigating climate and environmental changes in water basins [5,6] using bivalve mollusks shells [7–21]. Thus, shell's Mn:Ca ratio was applied for an analysis of the trophic state of the waterbodies [7], the Ba:Ca ratio allowed an assessment of the primary production of water ecosystems [22], and Sr:Ca ratio may reflect the temperature, salinity changes, and mussel growth rate [8,9,17,21]. For example, Sr:Ca ratio in the freshwater mussel *Lampsilis cardium* shell was related to the concentration of Sr in water, whereas this ratio in marine mussel *Mesodesma donacium*, *Chione subrugosa* [9], and *Pecten maximus* [19] depended on the shell's growth rate. It has been demonstrated that Mn:Ca ratio in bivalve shells can indicate the level of dissolved Mn^{2+} [7] and could be related to anoxic conditions below the clay bottom surface. Marine blue mussels *Mytilus edulis* exhibited seasonal fluctuations of Mn:Ca ratio, related to physiological control [23].

However, although these indicators allow to reconstruct various environmental controls, simultaneous application of these geochemical indicators for both marine and freshwater mussels have not been attempted. At the same time, the information on trace element composition of shells coupled to that of relevant environmental compartments (water and bottom sediments) may help to better understand element accumulation processes by mollusks in the mixing zone between the river and the sea. Towards this goal, here, we assessed multielemental (25 major and trace elements) composition of carbonate shells from marine and freshwater mussels that inhabited similar subarctic/boreal climate conditions. Given that the variations in metal concentration in the river are much stronger than those in the sea, we hypothesize essentially external (environmental, seasonal) control of trace element uptake by freshwater mussel shells and more stable, biologically-controlled pattern of trace element accumulation in shells of marine bivalves. To test this hypothesis, we compared trace element composition in marine and freshwater mussel shells on the basis of several environmental indicators, considering two contrasting sites across Northern Eurasia, one in the European Subarctic and another one in the Kamchatka Peninsula. The selected regions are well-studied in the course of fresh- and brackish-water mollusks and there are several well-known localities of widely distributed freshwater (*Unio* sp., *Anodonta* sp., and *Beringiana* sp.) and brackish-water (*Mytilus* sp.) species of mussels [24,25]; those were used in the presented study as representative sampling sites.

2. Methods

2.1. Sampling

Shells were collected by hand from the depth of 0.3 to 2.0 m in the Eastern and Western part of Northern Eurasia (Figure 1). List of studied localities is provided in Table 1. River water was collected at the site of shells' sampling, by one sample from each site, from 0.5 m depth. The water was immediately filtered through a single-use sterile acetate cellulose filter (Sartorius, 0.45 μ m) into pre-cleaned polypropylene Nalgene bottles. Filtered water samples for trace element analyses were acidified with ultrapure double-distilled HNO_3 and stored in the refrigerator pending analyses. The sediment samples were taken from the water-sediment interface, by one sample from each site, encompassing 0–4 cm layer, which corresponded to the depth of burying of *Anodonta anatina*, *Beringiana beringiana* and *Unio* mollusks in the substrate. Samples were placed in sterile double-zip polyethylene bags, preserved in cold dark environment, and transported within several days to the laboratory where they were dried at 90 °C in the oven.

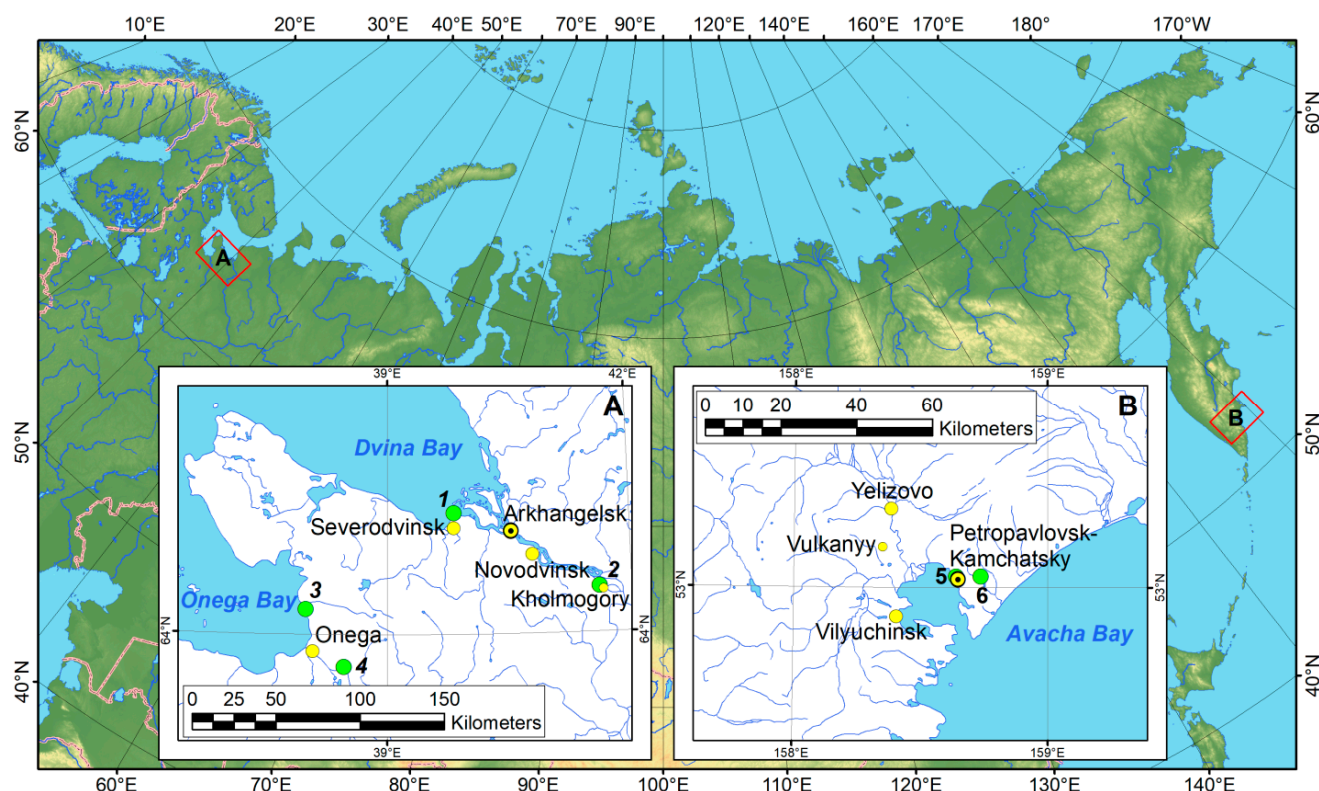


Figure 1. Map of the study sites: (A) White Sea Basin: 1—Jagry Island, Dvina Bay; 2—Severnaya Dvina River near Kholmogory village; 3—Onega Bay near Tamica River mouth; 4—Onega River near Porog village; (B) Pacific Ocean Basin: 5—Avacha Bay in Petropavlovsk-Kamchatskiy; 6—Khakaktyskoe Lake, Khalaktyrka River Basin.

Table 1. List of studied localities.

Environment	Locality	Species	Salinity (Marine Biotopes)/TDS (Freshwater Biotopes), g/L	Coordinates	
				Latitude	Longitude
Marine	Jagry Island, Dvina Bay	<i>Mytilus edulis</i>	6.13	64.643775 N	39.826407 E
	Onega Bay near Tamica River mouth	<i>Mytilus edulis</i>	7.01	64.134958 N	38.002934 E
	Avacha Bay in Petropavlovsk-Kamchatskiy	<i>Mytilus trossulus</i>	11.3	53.027181 N	158.640503 E
Freshwater	Severnaya Dvina River near Kholmogory village	<i>Unio pictorum</i> , <i>Anodonta anatina</i>	0.09	64.244167 N	41.608056 E
	Onega River near Porog village	<i>Unio tumidus</i> , <i>Anodonta anatina</i>	0.07	63.828889 N	38.475556 E
	Khakaktyskoe Lake, Khalaktyrka River Basin	<i>Beringiana beringiana</i>	0.04	53.027363 N	158.736206 E

2.2. Species Determination

The primary identification of collected bivalve mollusks was carried out based on standard and special keys [24,25]. The comparative analysis of the shell morphology was carried out, taking into account the structure of the pseudocardinal and lateral teeth, muscle attachment scars, shell shape, and umbo position [26,27]. Details of the shell structure were studied using an Axio Lab.A1 light microscope (Carl Zeiss, Jena, Germany) and a Leica M165C stereomicroscope (Leica Microsystems, Wetzlar, Germany).

2.3. Molecular Analyses

Total genomic DNA was extracted from free 96% ethanol-preserved sample mussels using the NucleoSpin Tissue Kit (Macherey-Nagel GmbH & Co. KG, Düren, Germany), following the manufacturer's protocol. For molecular analyses, we obtained sequences of the COI mitochondrial marker, which is widely used in such studies [28,29]. The COI sequences were amplified by a polymerase chain reaction (PCR) using the following primers: LCO1490 and HCO2198 [30] for *Mytilus edulis*, *Beringiana beringiana*, *Anodonta anatina*, and *Unio* sp., and Lobo F/2329 for *Mytilus trossulus*, respectively. The PCR mix contained approximately 200 ng of total cell DNA, 10 pmol of each primer, 200 pmol of each dNTP, 2.5 µl of PCR buffer (with 10×2 mmol MgCl), and 0.8 units Taq DNA polymerase (SibEnzyme Ltd., Novosibirsk, Russia), and H₂O was added for a final volume of 25 µl. Thermocycling was implemented with marker-specific PCR programs as follows: 95 °C (5 min), followed by 32 cycles at 95 °C (45 s), 48–49 °C (40 s), 72 °C (50 s), and a final extension at 72 °C (5 min). Forward and reverse sequencing were performed on an automatic sequencer (ABI PRISM3730, Applied Biosystems, Waltham, USA) using the ABI PRISM BigDye Terminator version 3.1 reagent kit. The resulting sequences were checked using a sequence alignment editor BioEdit version 7.2.5 [31]. The nucleotide sequences of the bivalves were identified using the Basic Local Alignment Search Tool, BLAST [32].

2.4. Preparation of Shells to Chemical Analyses

For the analysis of major and trace elements, parts of the shell were cut within the place of the maximal growth, from umbo towards the edges (Figure 2A,C). We analyzed from four to six mussel specimens from each locality. The samples were washed using MilliQ water, dried, and ground in an agate mortar following standard preparation procedures [3,33].

2.5. X-ray Diffraction Analysis

Crystalline structure of shell's minerals was characterized using an XRD-7000S X-ray diffractometer (Shimadzu Corp., Kyoto, Japan) equipped with an attachment for sample rotation and a polycapillary optical system. The X-ray tube with a Cu target and a maximum power of 2 kW was used. The goniometer characteristics are as follows: θ – θ optical scheme, a scintillation detector with a monochromator adjusted to a wavelength of 1.5406 Å (CuK $_{\alpha 1}$ line). X-ray diffraction patterns of powder samples were registered on reflection mode with a standard holder (Al) at a rotation frequency of 30 rpm. The X-ray tube voltage was 50 kV and current 30 mA. The 2θ angle scanning was performed in the range of 10–150° at a scanning rate of 2 deg min^{−1} and a step of 0.020°. Quantitative analyses of mineral phases were performed with the Profex v. 5.0 software and its BGMN database.

2.6. Analysis of the Trace Element Composition of Shells, Water, and Bottom Sediment Samples

Mineralization of shell and sediment samples was carried out by acid digestion in Teflon Savillex vials. About 100 mg were used for analysis. Together with the analyzed samples, three blanks (without powder) and one certified standard material were digested. For control of the chemical yield during the sample decomposition procedure, to the aliquot of powder, we added 0.1 mL of a solution containing ¹⁴⁵Nd, ¹⁶¹Dy, and ¹⁷⁴Yb (8 µg/dm³), moistened with several drops of deionized water. Then, 0.5 mL of HClO₄ (Perchloric acid fuming 70% Supratur, Merck, Rahway, NJ, USA), 3 mL of HF (Hydrofluoric acid 40% GR, ISO, Merck), and 0.5 mL of HNO₃ (ultrapure, 65%, GR, ISO, Merck) were added and evaporated to intense white fumes, followed by cooling and washing from the vial walls. The residual solution was evaporated to wet salts. After that, 2 mL of HCl (ultrapure, fuming 37% GR, ISO, Merck) and 0.2 mL of 0.1 M H₃BO₃ solution (analytical grade) were added and the mixture was evaporated to a volume of 0.5–0.7 mL. The resulting solutions were transferred into pre-cleaned HDPE (high-density polyethylene) vials, into which 0.1 mL internal standard (10 mg/L of In) was added and diluted with 2% HNO₃ to 20 mL. The concentrations of Li, Be, Sc, Ti, V, Cr, Mn, Co, Ni, Cu, Zn, Ga, As, Se, Rb, Sr, Y, Zr, Mo, Nb, Ag, Cd, Sn, Sb, Cs, Ba, REEs, Hf, W, Tl, Pb, Bi, Th, and U were determined by

ICP-MS (X-7, Thermo Scientific, Waltham, USA), which operated in He and no-gas mode. To control the accuracy of analyses of mussels' shells' elemental composition, in parallel with the samples, we processed two certified carbonate reference materials (Coral JCp-1, Giant Clam JCt-1).

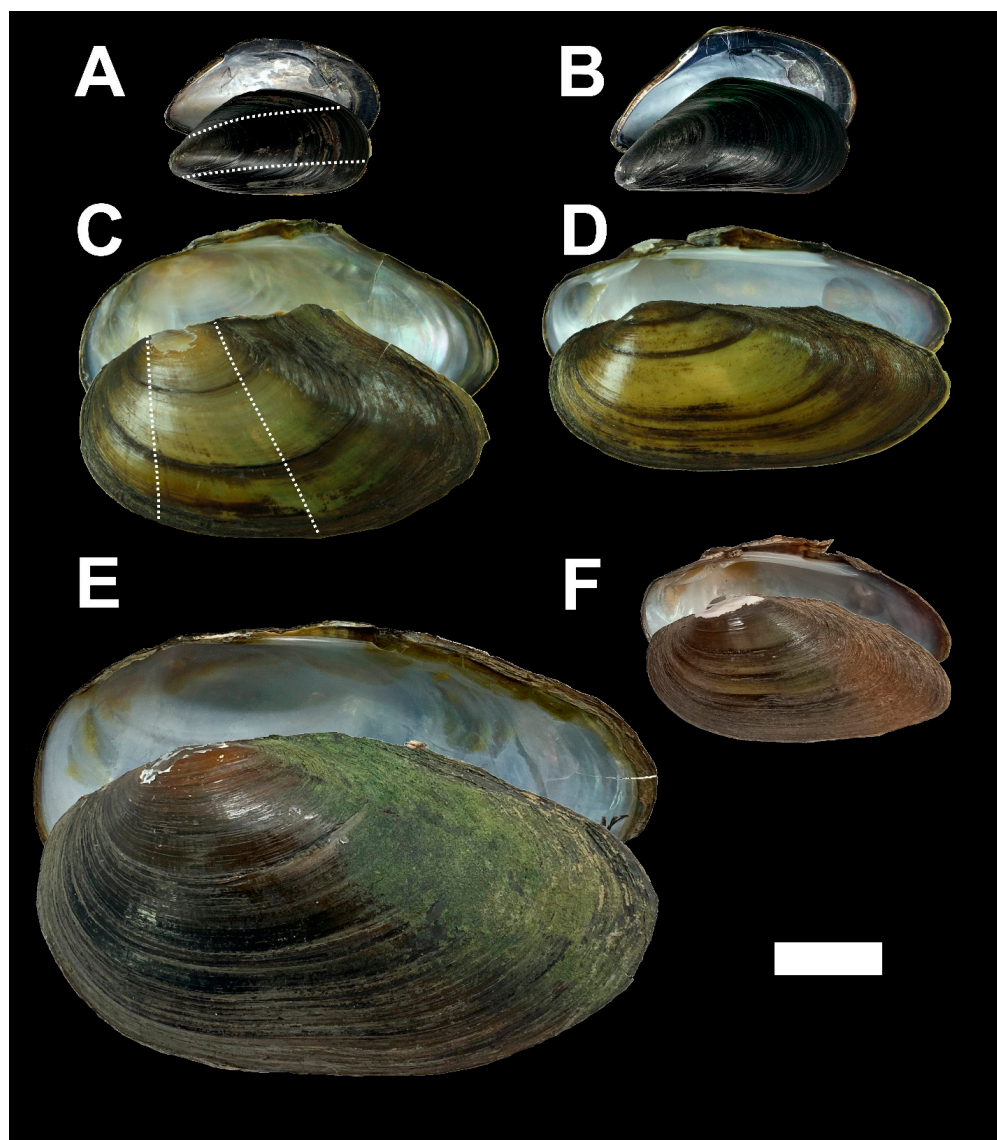


Figure 2. Shells of the studied species of marine and freshwater bivalve mollusks: (A)—*M. edulis*, the Onega Bay near the mouth of the Tamica River; (B)—*M. trossulus*; (C)—*A. anatina*, the Severnaya Dvina River near Kholmogory village; (D)—*U. pictorum*, the Severnaya Dvina River near Kholmogory village; (E)—*B. beringiana*, Khakaktyrskoe Lake, Khalaktyrka River Basin; (F)—*U. tumidus*, the Onega River near Porog village. Scale bar = 20 mm. White dashed lines show sampling places of material for chemical analyzes.

Freshwater and seawater samples were 0.45 μm filtered on-site and immediately acidified with concentrated ultrapure HNO_3 to 2%. Estuarine and seawater was diluted 10 to 40 times before analysis. The elemental composition of the water (Li, B, Na, Mg, Al, Si, P, S, K, Ca, Sc, Ti, V, Cr, Mn, Fe, Co, Ni, Cu, Zn, Ga, Ge, As, Se, Rb, Sr, Ba, Y, Zr, Nb, Mo, Cd, Sn, Sb, Cs, Ba, REE, Hf, W, Tl, Pb, Bi, Th, and U) was measured by ICP-AES. The detection limits of the method are presented in Supplementary Materials. Certified reference materials of natural riverine and estuarine water (SLRS-6 and SLEW-3, respectively) were used to monitor the accuracy of analyses.

In this study, we discuss only elements Li, Na, Mg, Al, P, S, K, Ca, Mn, Ti, V, Fe, Cu, Zn, As, Sr, Zr, Ba, La, Ce, Pr, Nd, Gd, Pb and U, which exhibited reasonable (10 to 20%) agreement with concentrations in certified international materials (carbonate solid phase, estuarine water, and river water). These elements represent labile cations (alkali and alkaline-earth metals), anions (S as sulfate and P as phosphate), trace metals such as micronutrients (V, Mn, Fe, Cu, and Zn), and pollutants (As and Pb), as well as low-mobile geochemical indicators (Al, Ti, Zr, REE, and U).

2.7. Data Treatment

2.7.1. Normality Tests and Comparisons

In addition to processing direct element concentrations, the values were normalized to Ca and Al concentrations. Normality for each analyzed sample was determined based on Shapiro–Wilk’s test significance values ($p > 0.05$). The Mann–Whitney U test was used to assess the differences between the concentrations in shell, water, and sediment samples. The Kruskal–Wallis H test was used for the measurement of the differences between the content of chemical elements in bivalve mollusk shells in several samples, and these data were ranked. Ranking consisted of the transition from the quantitative values of the concentrations of chemical elements to the ranks, which were subsequently compared with each other. Statistical analyses were carried out with use of STATISTICA software, version 10 (StatSoft Inc., Tulsa, OK, USA, 2011).

2.7.2. Pairwise and Multiple Linear Regression

Pairwise regression models were calculated in Microsoft Excel 2010 using the Analysis ToolPak. Significance of each model was estimated by F-test at $p < 0.05$. Multiple linear regression analysis was carried out with stepwise variable inclusion and with the multicollinearity test, with the outlier test, and with the Shapiro–Wilk normality test. We included in the analysis independent variables with the maximum correlation coefficient. Relationships between variables were assessed by values of the semi-partial correlation, which indicated part of influence for each independent variable.

2.7.3. Principal Component Analysis (PCA)

PCA was used to determine the factors controlling the pattern of element accumulation in shells, water, and sediments. The selection of factors was carried out according to the screen test and on the basis of eigenvalues (the Kaiser criterion). The suitability of the data for factorization was assessed based on the Kaiser–Meier–Olkin measure of sample adequacy (minimum fitness value was higher than 0.5) and using the Bartlett’s test of sphericity ($p < 0.05$).

2.7.4. General Linear Model (GLM)

General linear model (GLM) was used for identification of factors controlling accumulation of trace elements in different environments. Environmental factor was established for each model as independent categorical variable. Concentrations of trace elements were included in the model as dependent variables. Significance of relationship between factor and dependent variable(s) were estimated based on significance of Wilks’ lambda criterion ($p < 0.05$). Significance of model and strength of relationship between factor and each of dependent variables were assessed using R^2 and probability values with the upper level at $p < 0.01$.

2.7.5. Metal Pollution Index (MPI)

The MPI was calculated according to Usero et al. [34] and Sedeño-Díaz et al. [35] based on following equation:

$$\text{MPI} = (M_1 \times M_2 \times M_3 \times \dots \times M_n)^{1/n},$$

where MPI is the metal pollution index, M_i is the concentration of the i^{th} metal, and n is the number of analyzed metals. Typically, the MPI was assessed based on Li, Na, Mg, Al, P, K, Ti, Mn, Fe, Cu, Zn, Sr, Zr, Ba, La, Ce, Pr, Nd, Gd, Pb, and U concentrations in shells or sediments.

3. Results

3.1. Species Determination

3.1.1. Collected Mollusks' Samples and Shell Structure

The collected shells of bivalve mollusks belonged to three freshwater (*Anodonta*, *Unio*, and *Beringiana*) and one marine genera (*Mytilus*) (Figure 2). All analyzed individuals of *Anodonta* belonged to the species *A. anatina*. The individuals belonging to the genus *Unio*, according to the teeth structure and the outline of the shell contours, were identified as *U. pictorum* and *U. tumidus*. The average ontogenetic ages of individuals were 4.17 ± 0.20 years for specimens of *Anodonta* and 4.67 ± 0.20 years for specimens of *Unio*. All individuals of genus *Beringiana* were identified as ones belonging to mussel species *B. beringiana*. The average ontogenetic ages of *B. beringiana* were 6.30 ± 1.02 years. The analyzed individuals of blue mussels *Mytilus* belonged to the species *Mytilus edulis* and *Mytilus trossulus*. The average ontogenetic ages of individuals were 4.0 ± 0.4 years for specimens of *Mytilus edulis* from the Dvina Bay, 5.0 ± 0.5 years for specimens of *Mytilus edulis* from the Onega Bay, and 5.6 ± 0.3 years for specimens of *Mytilus trossulus* from the Avacha Bay.

3.1.2. Molecular Analyses

Analyses of seven COI gene sequences for marine mussels with length of 663 bp demonstrated that the mollusk specimens belong to species *M. edulis* and *M. trossulus*. Analyses of five nucleotide sequences of COI gene for freshwater mussels with length of 660 bp yielded *B. beringiana*, *A. anatina*, *U. tumidus*, and *U. pictorum* specimens at the species level, in accordance with conchological features [25].

3.2. Mineralogical Composition of Shells

The shells of freshwater *A. anatina*, *Unio* sp., and *B. beringiana* consisted essentially of aragonite (>95%). At the same time, shells of marine mussels exhibited a sizable proportion (55–70%) of calcite (Table 2). Additionally, both marine and freshwater samples contained several percents of vaterite. The minimal mean percentage of vaterite was found for shells of marine species *Mytilus trossulus*, and the maximal one was measured for freshwater mussel *Anodonta anatina*.

Table 2. Mineralogical composition of the bivalve shells.

Species (Marine/Freshwater)	N	Calcite, %	Aragonite, %	Vaterite, %
<i>Mytilus edulis</i> (marine)	9	57.9 ± 3.1	39.1 ± 3.0	3.10 ± 0.15
<i>Mytilus trossulus</i> (marine)	5	67.0 ± 3.4	30.5 ± 3.0	2.46 ± 0.43
<i>Beringiana beringiana</i> (freshwater)	5	0.23 ± 0.11	95.6 ± 0.2	4.14 ± 0.14
<i>Anodonta anatina</i> (freshwater)	5	0.19 ± 0.07	95.5 ± 0.2	4.28 ± 0.18
<i>Unio</i> sp. (freshwater)	4	0.52 ± 0.28	95.6 ± 0.1	4.17 ± 0.10

3.3. Elemental Composition of Shells

The average chemical composition of marine and freshwater mollusk shells was dominated, after Ca, by Na, Sr, Mg, S, P, Fe, and Mn (Figure 3A). Average concentrations of Na, Sr, Mn, Fe, and P in marine ($n = 14$) and freshwater ($n = 15$) shells were 3350 ± 109 and 2250 ± 54 , 1370 ± 46 and 434 ± 50 , 63.1 ± 24.8 and 521 ± 47 , 152 ± 44 and 989 ± 220 , and 158 ± 6.1 and 140 ± 23 ppm, respectively (Tables S1 and S2). Na, Sr, Mg, S, P, Zn, Li, and U were generally more abundant in shells from marine coastal environments

compared to freshwater ones. The second group of elements included Fe, Mn, K, Al, Ba, Ti, and Cu, whose concentrations were higher in freshwater compared to marine mollusk shells (Figure 3B, Table 3). Al-normalized concentrations of most elements were higher in marine mussels (Mann–Whitney criterion, $p > 0.05$) (Figure 4A).

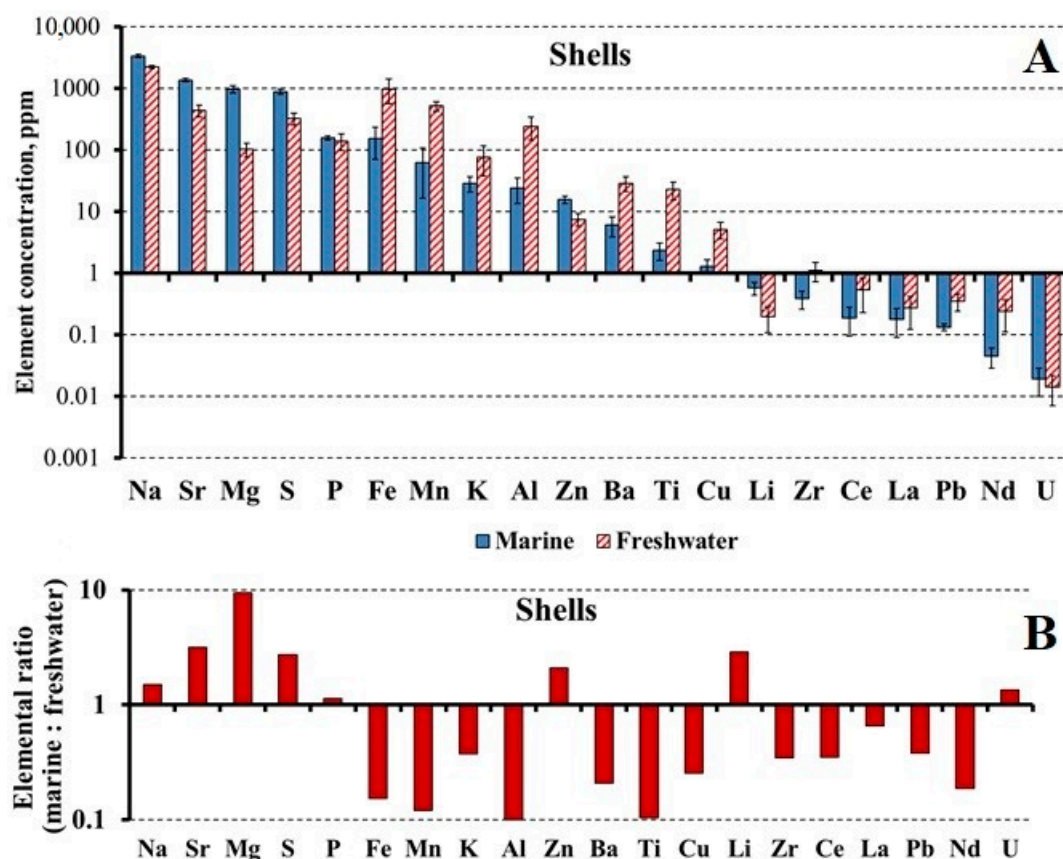


Figure 3. (A)—mean concentrations of trace elements in bivalve shells: blue columns, marine mussels ($N = 14$), and hatched columns, freshwater mussels ($N = 14$). Error bars indicate s.e.m.; (B)—Ratios of element mean concentrations in shells of marine to freshwater bivalve.

Upper-crust normalized REE concentrations in the shells did not exhibit significant differences between marine and freshwater samples ($p > 0.01$), except for Nd and Gd ($p < 0.01$) (Figure S1). Concentrations of La, Ce, Pr, Nd, and Gd in the shells normalized to their concentrations in the sediment did not demonstrate significant differences ($p > 0.05$) between marine and freshwater samples, although, in marine settings, concentrations of Pr, Nd, and Gd were sizably lower in shells compared to sediments (Figure S2).

3.4. Elemental Composition of Water and Bottom Sediments

The concentrations of chemical elements in water and bottom sediments (Table S3) revealed two groups of elements: (1) Na, K, B, S, Mg, Cs, Rb, Sr, U, and Mo, which dominated in marine biotopes; and (2) Ca, Al, and Mn, which were related to freshwater biotopes (Figure S3). For example, the mean ratios between trace element concentrations in marine and fresh water samples varied from 2.6 ± 1.5 and 3.7 ± 2.8 for Mn and Al, respectively, to 190 ± 38 and 790 ± 200 for K and Na, respectively. S, Na, Ba, K, Sr, and P dominated elemental composition of bottom sediments in marine environments, whereas Al, Mg, Li, Ca, Mn, Fe, Zn, Ti, Pb, and V dominated in sediments from freshwater environments (Figure 4B). Thus, mean ratio of trace element concentrations in sediment samples from marine to freshwater localities varied from 0.34 ± 0.22 for V to 2.49 ± 1.97 for S.

Table 3. Elemental composition of mussels' shells from studied localities: n.d.—not determined.

Element	<i>Anodonta anatina</i> , Severnaya Dvina River near Khol- mogory Village, Mean \pm SE, ppm ($n = 2$)	<i>Unio</i> sp., Severnaya Dvina River near Khol- mogory Village, Mean \pm SE, ppm ($n = 2$)	<i>Anodonta anatina</i> , Onega River near Porog Village, Mean \pm SE, ppm ($n = 2$)	<i>Unio</i> sp., Onega River near Porog Village, Mean \pm SE, ppm ($n = 2$)	<i>Beringiana beringiana</i> , Khakaktyrskoe Lake, Kha- laktyrka River Basin, Mean \pm SE, ppm ($n = 5$)	<i>Mytilus edulis</i> , Jagry Island, Dvina Bay Mean \pm SE, ppm ($n = 4$)	<i>Mytilus edulis</i> , Onega Bay near Tamica River Mouth Mean \pm SE, ppm ($n = 5$)	<i>Mytilus trossulus</i> , Avacha Bay in Petropavlovsk- Kamchatkiy Mean \pm SE, ppm ($n = 5$)
Li	0.25 \pm 0.14	0.15 \pm 0.01	0.36 \pm 0.10	0.35 \pm 0.07	n.d.	0.38 \pm 0.02	0.41 \pm 0.05	0.90 \pm 0.05
Na	2540 \pm 127	2400 \pm 76	2380 \pm 67	2010 \pm 41	2140 \pm 43	3450 \pm 191	3100 \pm 235	3520 \pm 92
Mg	114 \pm 59	78.2 \pm 2.8	161 \pm 46	84.8 \pm 17.9	85.6 \pm 12.2	1020 \pm 65	1210 \pm 90	700 \pm 14
Al	368 \pm 211	139 \pm 8.8	428 \pm 161	241 \pm 73	121 \pm 26	34.5 \pm 9.1	36.3 \pm 9.5	n.d.
P	203 \pm 121	202 \pm 120	72.2 \pm 10.6	109 \pm 16.3	150 \pm 26	154 \pm 12	153 \pm 7.1	167 \pm 13
S	332 \pm 133	227 \pm 51	223 \pm 59	231 \pm 22	478 \pm 44	737 \pm 30	892 \pm 83	1010 \pm 71
K	149 \pm 97	56.9 \pm 1.5	148 \pm 54	78.2 \pm 23.8	12.6 \pm 2.4	31.8 \pm 11.3	36.1 \pm 6.6	19.1 \pm 3.73
Ca	399,000 \pm 6000	376,000 \pm 10,000	394,000 \pm 2600	384,000 \pm 1270	397,000 \pm 6930	406,000 \pm 9400	423,000 \pm 4310	385,000 \pm 10,800
Ti	43.3 \pm 13.3	17.9 \pm 0.53	31.9 \pm 11.2	16.3 \pm 3.9	14.6 \pm 2.4	2.41 \pm 0.74	2.97 \pm 0.89	n.d.
Mn	594 \pm 79	327 \pm 10	390 \pm 33	459 \pm 97	685 \pm 75	154 \pm 71	41.7 \pm 12.3	12.2 \pm 1.3
Fe	1780 \pm 1310	1470 \pm 946	557 \pm 157	1130 \pm 451	655 \pm 191	337 \pm 100	105 \pm 37	51.5 \pm 9.4
Cu	2.90 \pm 0.32	2.05 \pm 0.11	3.54 \pm 0.32	3.48 \pm 0.68	9.22 \pm 0.34	0.96 \pm 0.23	0.92 \pm 0.23	1.96 \pm 0.25
Zn	2.38 \pm 2.14	3.63 \pm 0.89	9.99 \pm 1.76	10.3 \pm 1.27	7.9 \pm 0.68	17.3 \pm 2.13	16.0 \pm 2.1	14 \pm 1.4
Sr	774 \pm 41	671 \pm 49	370 \pm 3.8	399 \pm 19	263 \pm 9.6	1600 \pm 37	1340 \pm 19	1210 \pm 35
Zr	1.83 \pm 0.70	0.54 \pm 0.11	1.91 \pm 0.61	1.08 \pm 0.11	0.59 \pm 0.03	0.42 \pm 0.14	0.4 \pm 0.1	0.34 \pm 0.14
Ba	54.5 \pm 14.9	38.0 \pm 13.3	28.1 \pm 1.82	28.4 \pm 3.92	15.5 \pm 1.53	12.2 \pm 1.01	4.44 \pm 0.32	2.69 \pm 0.13
La	0.68 \pm 0.42	0.42 \pm 0.18	0.29 \pm 0.09	0.29 \pm 0.11	0.02 \pm 0.01	0.11 \pm 0.02	0.38 \pm 0.06	0.031 \pm 0.003
Ce	1.39 \pm 0.90	0.73 \pm 0.33	0.58 \pm 0.19	0.64 \pm 0.26	0.03 \pm 0.01	0.15 \pm 0.04	0.39 \pm 0.04	n.d.
Pr	0.17 \pm 0.09	0.09 \pm 0.03	0.07 \pm 0.02	0.07 \pm 0.02	0.006 \pm 0.001	0.02 \pm 0.01	0.011 \pm 0.002	0.009 \pm 0.004
Nd	0.62 \pm 0.39	0.33 \pm 0.15	0.26 \pm 0.09	0.27 \pm 0.11	0.03 \pm 0.01	0.08 \pm 0.02	0.05 \pm 0.01	0.013 \pm 0.004
Gd	0.10 \pm 0.06	0.06 \pm 0.04	0.04 \pm 0.02	0.04 \pm 0.02	0.013 \pm 0.002	0.018 \pm 0.002	0.010 \pm 0.001	0.005 \pm 0.001
Pb	0.54 \pm 0.10	0.40 \pm 0.05	0.25 \pm 0.08	0.55 \pm 0.22	0.20 \pm 0.02	0.11 \pm 0.01	0.12 \pm 0.01	0.165 \pm 0.009
U	0.04 \pm 0.02	0.013 \pm 0.004	0.02 \pm 0.01	0.02 \pm 0.01	n.d.	0.008 \pm 0.004	0.012 \pm 0.003	0.04 \pm 0.01

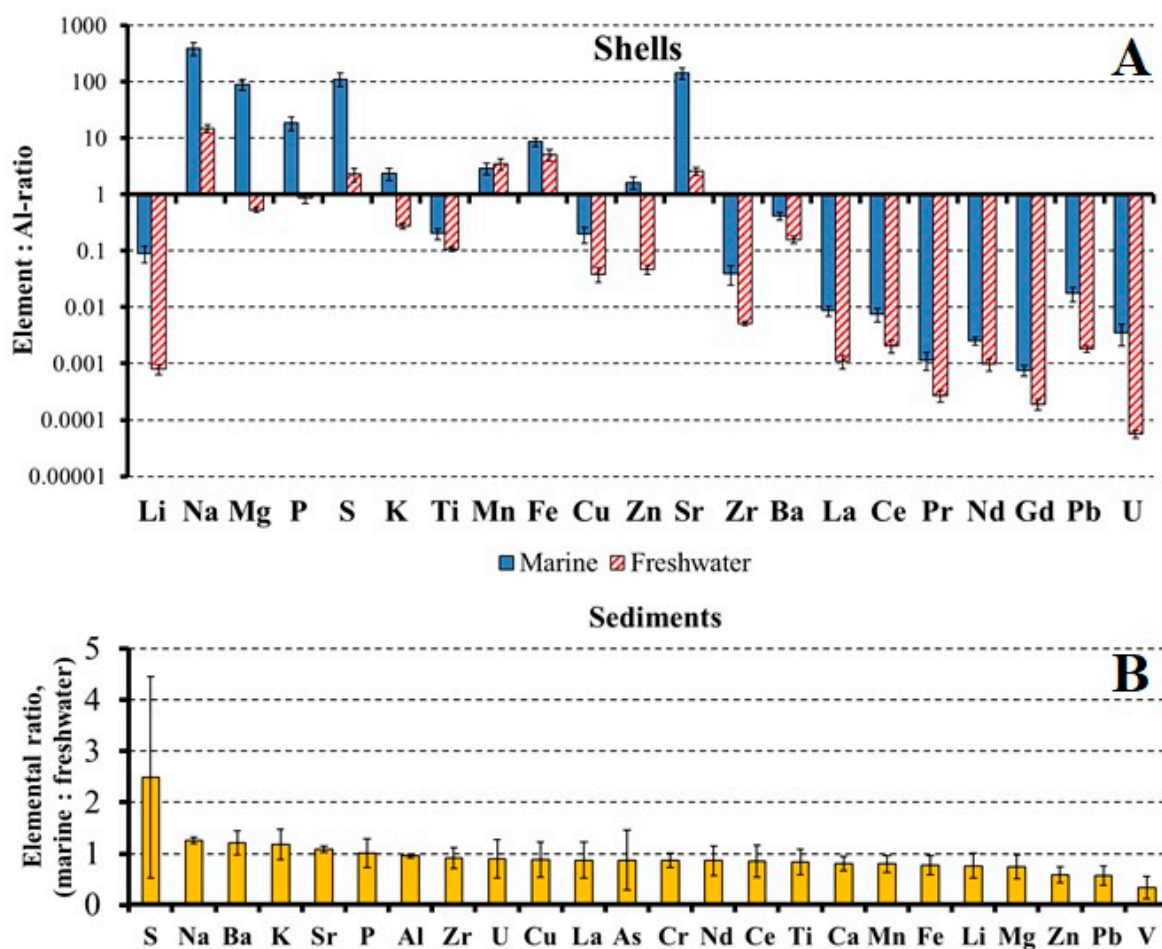


Figure 4. (A)—Mean Al-normalized concentrations of trace elements in bivalve shells: blue columns, marine mussels (N = 15), and hatched columns, freshwater mussels (N = 14). Error bars indicate s.e.m.; (B)—Mean ratio of trace elements concentrations in sediments of marine to freshwater localities. Error bars indicate s.e.m.

3.5. Element Distribution Coefficients between the Shell and the Environment

Apparent distribution coefficients of major and trace elements between the water and the CaCO_3 shells of freshwater and marine bivalve mollusks were calculated based on several replicates from the same site. Calcium-normalized distribution coefficients $K_d \text{ Shell/Water} = ([\text{TE}]/[\text{Ca}])_{\text{Shell}}/([\text{TE}]/[\text{Ca}])_{\text{Water}}$ between shells and water samples varied from 0.00003 for K to 21.6 for Mn (Table S4). Calcium-normalized distribution coefficients of trace elements between shells and bottom sediments ($K_d \text{ Shell/Sediment}$) ranged from 0.000006 for Al to 0.46 for Sr. The highest values of $K_d \text{ Shell/Water}$ were observed for freshwater mussels, where we determined $K_d \text{ Shell/Water}$ for Mn from 0.25 to 21.6, Sr from 0.15 to 0.25, Al from 0.10 to 4.24, and Na from 0.007 to 0.051. In marine mussels, we measured $K_d \text{ Shell/Sediment}$ for Mn from 0.12 to 4.38, Sr from 0.14 to 0.23, Al from 0.04 to 0.35, and Na from 0.0002 to 0.0004.

3.6. Statistical Treatment

3.6.1. Comparison of Marine and Freshwater Shell Samples by Elemental Ratios

The majority of studied trace elements exhibited an abnormal distribution of concentrations. Normal distribution among freshwater samples was found only for Na, Mn, and Zn. In marine shell samples, normal distribution was observed for Ti, Fe, Zr, Ba, U, Li, La, Ce, and Al. Comparison of Ca-normalized concentrations of Na, Mn, Mg, and Ba revealed significant ($p < 0.05$) differences among localities and species (Table S5). Ca-normalized

concentration of Sr differed among localities ($p < 0.05$), but they were not significant among species ($p > 0.05$). Freshwater species of mussels did not differ by Ca-normalized concentrations of Na and Mg ($p > 0.05$). Samples of freshwater mussels had significant differences by Ca-normalized concentrations of Na, Mn, Ba, and Sr among localities ($p < 0.05$). Freshwater species also differed by Ca-normalized concentrations of Mn, Ba, and Sr ($p > 0.05$).

Comparison of the Al-normalized concentration of Na, Ba, and Sr among species and among localities demonstrated that Na, Ba, Sr, and Mg differ by these two factors for freshwater mussels. At the same time, Na, Ba, and Sr did not differ among freshwater localities and species. The Al-normalized concentration of Mn in freshwater mussels' shells, on the contrary, demonstrated a difference by both of these factors.

Pairwise regression models allowed to check for the presence of the relationship between concentration of elements in shells and in the environmental compartments. Significant relationships ($p < 0.05$) were revealed between concentration in shells and water for Sr, Mg, Na, and S. Furthermore, significant correlations were also observed between Ca-normalized concentrations of Li, S ($p < 0.01$), and Na ($p < 0.05$) in shells and in water, whereas Ca-normalized concentrations of U in shells correlated to that in bottom sediment (Table S6).

3.6.2. Comparison of Al-normalized Concentration of Elements in Shells among Localities

Comparison of Al-normalized concentration of elements in mussels' shells demonstrated significant differences between different localities for Li, Na, Mg, P, S, K, Ca, Ti, Mn, Cu, Zn, Sr, Ba, REEs, Pb, U ($p < 0.01$), and for Fe ($p < 0.05$). The highest values of Al-normalized concentration were established for marine biotopes with the maximal concentration in the Avacha Bay. The lowest values were encountered for three freshwater sites. Significant differences in Al-normalized concentration of elements among three studied regions were determined for Li, Na, Mg, P, S, K, Ca, Zn, Sr, Ba, Zr, light REEs, Pb, and U ($p < 0.05$). There were no differences between the concentration of Ti, Mn, Fe, Cu, and Ce ($p > 0.05$). The highest concentrations of the four listed elements were estimated in biotopes in the Khalaktyrka River basin and the Avacha Bay. Al-normalized concentrations of Ti, Mn, and Fe had no significant differences between samples of marine and freshwater shells ($p > 0.05$). Al-normalized concentration of Li, Na, Mg, P, S, K, Ca, Ti, Mn, Fe, Cu, Zn, Sr, Zr, Ba, light REEs, Pb, and U differed between marine and freshwater samples ($p < 0.05$) with the highest values observed for marine shells.

3.6.3. PCA Treatment of Trace Element Concentrations and Distribution Coefficients

Preliminary assessment of the suitability of concentration data on Li, Na, Mg, Al, P, S, K, Ti, Mn, Fe, Cu, Zn, Sr, Zr, Ba, REEs, Pb, and U in shells for factorization revealed an acceptable value of the Kaiser–Mayer–Olkin sample adequacy measure (0.634), and a statistically significant indicator of Bartlett's sphericity criterion ($\chi^2 = 1174$; $p < 0.001$). Factor 1 and 2 explained 54.0% and 21.4% of the dispersion, respectively. These two factors were interpreted as follows, in terms of the values of factor loadings. Factor 1 was related to bottom sediments and accumulation of metals in shells, such as Al (0.879), K (0.815), Ti (0.928), Mn (0.698), Fe (0.873), Ba (0.947), and REEs (from 0.732 for La to 0.918 for Nd). Factor 2 could have a relationship with elemental composition of water due to its high loadings for labile elements such as Na (0.616), Mg (0.581), Sr (0.724), U (0.638), and S (0.528).

Assessment of suitability of Ca-normalized distribution coefficient of Li, Na, Mg, Al, S, K, Mn, Sr, and U between mussels' shell and water for factorization revealed the allowable value of the Kaiser–Mayer–Olkin sample adequacy measure (0.521) and a statistically significant indicator of Bartlett's sphericity criterion ($\chi^2 = 202$; $p < 0.001$). Two factors explained 64.3% of variance, including 40.6 and 23.7% for F1 and F2, respectively. Factor 1 was related to distribution coefficients of Li (0.843), Na (0.734), Mg (0.806), Al (0.778), and K (0.977), according to factor loadings. Factor 2 had strong correlations with S (0.894) and Mn (0.922).

We determined the suitability of data on Ca-normalized distribution coefficient of Li, Na, Mg, Al, P, S, K, Ti, Mn, Fe, Zn, Sr, Zr, Ba, REEs, and Pb between mussels' shell and bottom sediment for factorization based on value of the Kaiser–Mayer–Olkin sample adequacy measure (0.660) and a statistically significant indicator of Bartlett's sphericity criterion ($\chi^2 = 963$; $p < 0.001$). Two factors explained 63.6% of the total variance, including 44.2% and 19.4% for F1 and F2, respectively. Factor 1 was positively related to distribution coefficients of Al (0.902), Ti (0.917), Mn (0.872), Fe (0.811), Pr (0.818), Nd (0.931), and Gd (0.937). Factor 2 had positive correlation with distribution coefficient of Na (0.975) and moderate positive correlations with the distribution coefficients of Li (0.600), S (0.555), K (0.504), Sr (0.622), and Zr (0.562).

The Al-normalized trace elements' concentrations in mussels' shells were also suitable for factorization based on the value of the Kaiser–Mayer–Olkin sample adequacy measure (0.572) and a statistically significant indicator of Bartlett's sphericity criterion ($\chi^2 = 1874$; $p < 0.001$). Factor 1 explained 69.8% of variance, and factor 2 and factor 3 explained 10.6% and 7.5% of variance, respectively. Factor 1 had a strong correlation with Li (0.958), Na (0.984), Mg (0.975), P (0.968), S (0.991), K (0.907), Ca (0.986), Ti (0.938), Cu (0.909), Zn (0.969), Sr (0.992), Zr (0.769), Ba (0.883), Gd (0.828), Pb (0.977), and U (0.860). Factor 2 was positively related to distribution coefficients of La (0.798), Ce (0.883), and Nd (0.627). Factor 3 had positive correlation with the distribution coefficient of Fe (0.555).

3.7. Controlling Factors of Accumulation of Trace Elements in Mussels' Shells

General linear model (GLM) suggested a dependence of the trace element concentration in mussels' shells from several factors, including the type of environments (freshwater/marine), species identity, and locality. Therefore, it allowed to distinguish biological and environmental control on trace elements accumulation.

3.7.1. Biological Control (Species Identity)

Comparison of samples belonging to different species within marine and freshwater groups revealed the following elemental pattern: Four elements (Li, S, La, and U) exhibited significant relationships with the "species" identity factor ($p < 0.05$) among freshwater mussels (Table S7). Moderate relationships were revealed for S ($R^2 = 0.507$, $p < 0.006$) and Li ($R^2 = 0.523$, $p < 0.005$) by factor "species" among freshwater samples. Furthermore, Li, Na, Mg, S, La, Ce, Nd, Pb, and U had significant relationships (Wilk's λ criterion, $p < 0.05$) with the "species" factor among marine mussels. The highest significance of the influence of the "species" factor on the Ca-normalized concentration of elements was estimated for marine samples (Wilk's λ criterion, $p = 0.01$).

Further insights on Sr and Ba distribution in shells can be obtained via Ca-normalized concentrations which allowed to avoid the artifacts linked to matrix dilution. Ca-normalized concentrations of Sr in freshwater shells had stronger relationships with the factor "locality" ($R^2 = 0.962$, $p < 0.001$) compared to that in marine environments ($R^2 = 0.727$, $p < 0.001$) (Table S8). On the contrary, Ca-normalized concentrations of Ba in shells exhibited moderate relationships with this factor in freshwater environments ($R^2 = 0.590$, $p < 0.002$) and strong relationships in marine environments ($R^2 = 0.908$, $p < 0.001$).

Overall, among marine species, the biological control was evidenced for Li ($R^2 = 0.884$, $p < 0.001$), Mg ($R^2 = 0.602$, $p < 0.001$), Al ($R^2 = 0.507$, $p < 0.003$), Cu ($R^2 = 0.533$, $p < 0.002$), light REE (La–Nd; $0.4 < R^2 < 0.55$, $p < 0.005$), and Pb ($R^2 = 0.590$, $p < 0.001$, Table S7).

3.7.2. Environmental (Locality) Control

A number of elements in marine mussels' shells were controlled by the factor "locality" (geographical location of sampling points), including Li ($R^2 = 0.874$, $p < 0.001$), Sr ($R^2 = 0.727$, $p < 0.001$), Ba ($R^2 = 0.908$, $p < 0.001$), LREE ($0.6 < R^2 < 0.82$, $p < 0.001$), and Pb ($R^2 = 0.556$, $p < 0.005$). In mussels from freshwater biotopes, Cu ($R^2 = 0.935$, $p < 0.001$) and Sr ($R^2 = 0.962$, $p < 0.001$) concentrations had the strongest relationships with the factor "locality". Additionally, relationships with this factor were found for Li

($R^2 = 0.652$, $p < 0.005$), S ($R^2 = 0.541$, $p < 0.005$), and Ba ($R^2 = 0.590$, $p < 0.005$) (Table S8). Furthermore, Ca-normalized concentrations of Ba and Sr had significant relationships with the factor “locality”, being stronger for Sr and lower for Ba. In contrast, in the marine environments, the locality factor had stronger relationship with Ba and weaker with Sr.

General linear model analysis of samples from particular sampling sites based on the Al-normalized concentration of trace elements in freshwater mussels’ shells showed significant ($p < 0.01$) effect of the factor “locality” to variance of the elemental concentration (Table S9). The linear model revealed a significant influence of the geographical factor to variances in Cu and Li (73.2% and 69.6% of variance, respectively). Further, there were significant relationships with the factor “locality” for concentrations of S, Ti, Mn, Cu, Ce, Nd, and U in the shells of freshwater mussels ($p < 0.01$, Table S9).

In marine mussel’s shell, significant relationships with the factor “locality” were found for Al-normalized concentrations of Li, Na, Mg, S, K, Mn, Fe, Cu, Zn, Sr, Pr ($p < 0.01$), and Ba ($p < 0.05$). The factor locality determined more than 90% of the Al-normalized concentration variance for Li, Na, Mg, K, Zn, and Pr (Table S10). Additionally, Al-normalized concentration of Sr exhibited strong relationship with the factor “locality”, whereas that of Ba had weak relationships with this factor.

Distribution coefficient K_d Shell/Water of Li, S, Mn, and Sr was strongly related to the factor “locality” (Wilk’s λ criterion, $p < 0.01$, Table S11). The highest percentage of explained variance was observed for Mn ($R^2 = 0.91$, $p < 0.001$) and S ($R^2 = 0.894$, $p < 0.001$), whereas the values of K_d Shell/Water for Li ($R^2 = 0.551$, $p < 0.001$) and Sr ($R^2 = 0.616$, $p < 0.001$) exhibited weaker relationships with the “locality” factor.

3.7.3. Distribution Coefficients between Shells and Water in Marine and Freshwater Environment

The distribution coefficients of K, Na, Al, and Mn between shell and water were much higher for freshwater mussels compared to marine ones (Figure 5). Significant differences in K_d Shell/Water between marine and freshwater samples were observed for Na, Mg, and S (Mann–Whitney U test, $p < 0.001$), but not for Sr (Mann–Whitney U test, $p > 0.01$). For the K_d Shell/Sediments, significant differences between marine and freshwater samples were observed for Sr, Mg, and S, but not for Na. The strongest relationships ($p < 0.001$) between K_d Shell/Water and the identity of species were found for Na, S, and Mn (Table S12). More than 82% of these variables’ variances were explained by the biological (“species”) factor. Significant relationships ($p < 0.05$) were also observed for Mg, Al, and U. Overall, there was a power dependence between K_d Shell/Water of marine and freshwater mussels for Li, Na, Mg, Al, S, K, Mn, Sr, and U for freshwater and for marine mussels ($R^2 = 0.99$, $p < 0.001$) (Figure 6).

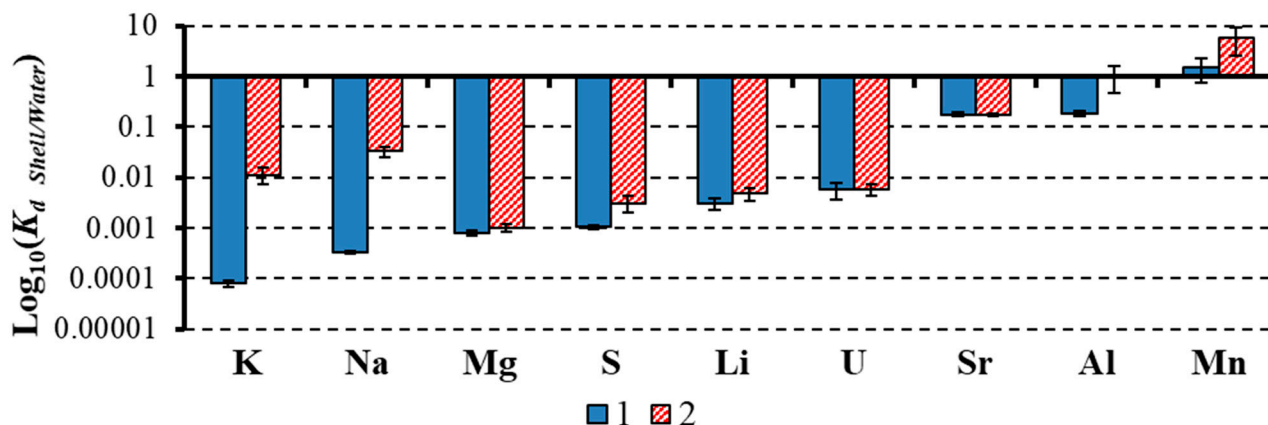


Figure 5. Calcium-normalized distribution coefficients (K_d) of elements between mollusks’ shells and water: 1—marine mussels (N = 15), 2—freshwater mussels (N = 14). Error bars indicate s.e.m.

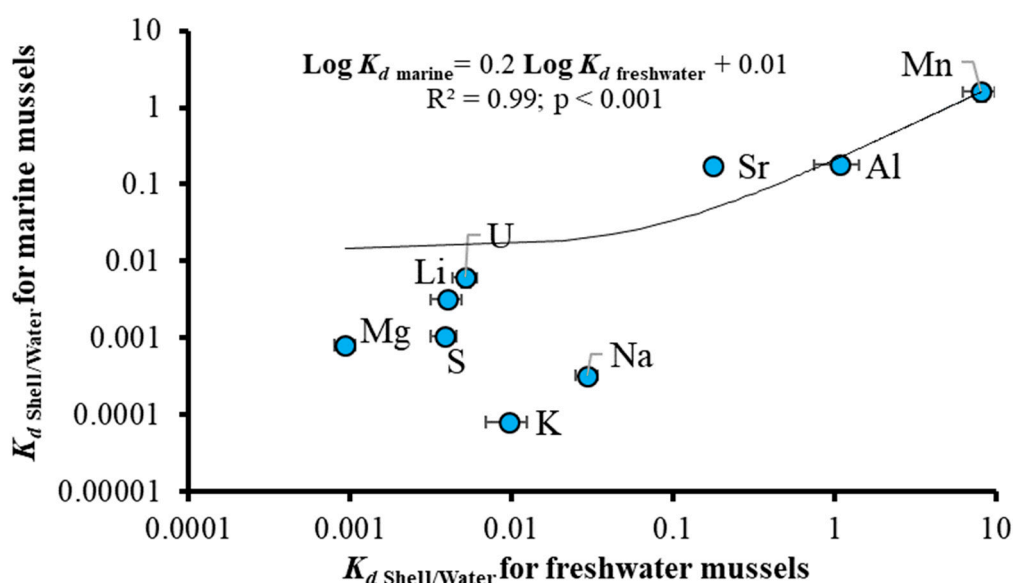


Figure 6. Relationships between mean values of distribution coefficients of elements K_d Shell/Water for samples from freshwater (X-axis) and marine (Y-axis) biotopes.

3.8. Mineralogical Control of Elemental Composition

Strong positive correlations were found between percentage of calcite in shells and Ca-normalized concentrations of Na, Mg, and Sr ($R_{\text{Spearman}} = 0.73\text{--}0.80$, $p < 0.01$, Table S13), whereas moderate positive correlation was observed between percentage of calcite in shells and Ca-normalized concentration of Zn ($R_{\text{Spearman}} = 0.62$, $p < 0.01$). We observed strong correlations between percentage of aragonite and vaterite in shells and the concentrations of Mn ($R_{\text{Spearman}} = 0.76\text{--}0.77$, $p < 0.01$), Fe ($R_{\text{Spearman}} = 0.69\text{--}0.75$, $p < 0.01$), Ti ($R_{\text{Spearman}} = 0.70\text{--}0.77$, $p < 0.01$), and Ba ($R_{\text{Spearman}} = 0.75\text{--}0.81$, $p < 0.01$); moderate correlations between percentage of aragonite and vaterite in shells and Ca-normalized concentrations of Gd, Zr, Cu, and Pb ($R_{\text{Spearman}} = 0.54\text{--}0.68$, $p < 0.01$); a moderate correlation between percentage of vaterite in shells and the concentration of Nd ($R_{\text{Spearman}} = 0.58$, $p < 0.05$); weak correlations between vaterite percentage and Ca-normalized concentrations of Ce and Pr ($R_{\text{Spearman}} = 0.38\text{--}0.43$, $p < 0.05$); and weak correlation between percentage of aragonite in shells and the Ca-normalized concentration of Nd ($R_{\text{Spearman}} = 0.45$, $p < 0.05$).

We found strong positive correlations between percentage of calcite in shells and Al-normalized concentrations of Na, Mg, Sr, Zn, La, and Pb ($R_{\text{Spearman}} = 0.73\text{--}0.82$, $p < 0.01$, Table S14); moderate positive correlations between calcite percentage and Al-normalized concentrations of Ba, Pr, Nd, and Gd ($R_{\text{Spearman}} = 0.55\text{--}0.65$, $p < 0.01$); and weak positive correlations between percentage of calcite and Al-normalized concentrations of Fe, Cu, and Ce ($R_{\text{Spearman}} = 0.38\text{--}0.40$, $p < 0.05$). In contrast, aragonite and vaterite content in shells did not exhibit any discernable control on Al-normalized element concentrations. Further, the distribution coefficient of Mn between shell and sediment has significant regression relationships with vaterite percentage in studied bivalve shells ($R^2 = 0.61$, $p < 0.001$, Figure 7A).

3.9. Metal Pollution Index

The metal pollution index (MPI) varied from 1.42 to 5.05 for marine mussels *Mytilus* spp. and from 1.93 to 15.2 for freshwater mussels from genera *Anodonta*, *Unio*, and *Beringiana* (Figure S4). The MPI demonstrated statistically significant differences between three geographic regions for both marine and freshwater species (Kruskal–Wallis criterion, $p < 0.001$, Figure S4A) and among all studied species of mussels (Kruskal–Wallis criterion, $p < 0.0005$, Figure S4B).

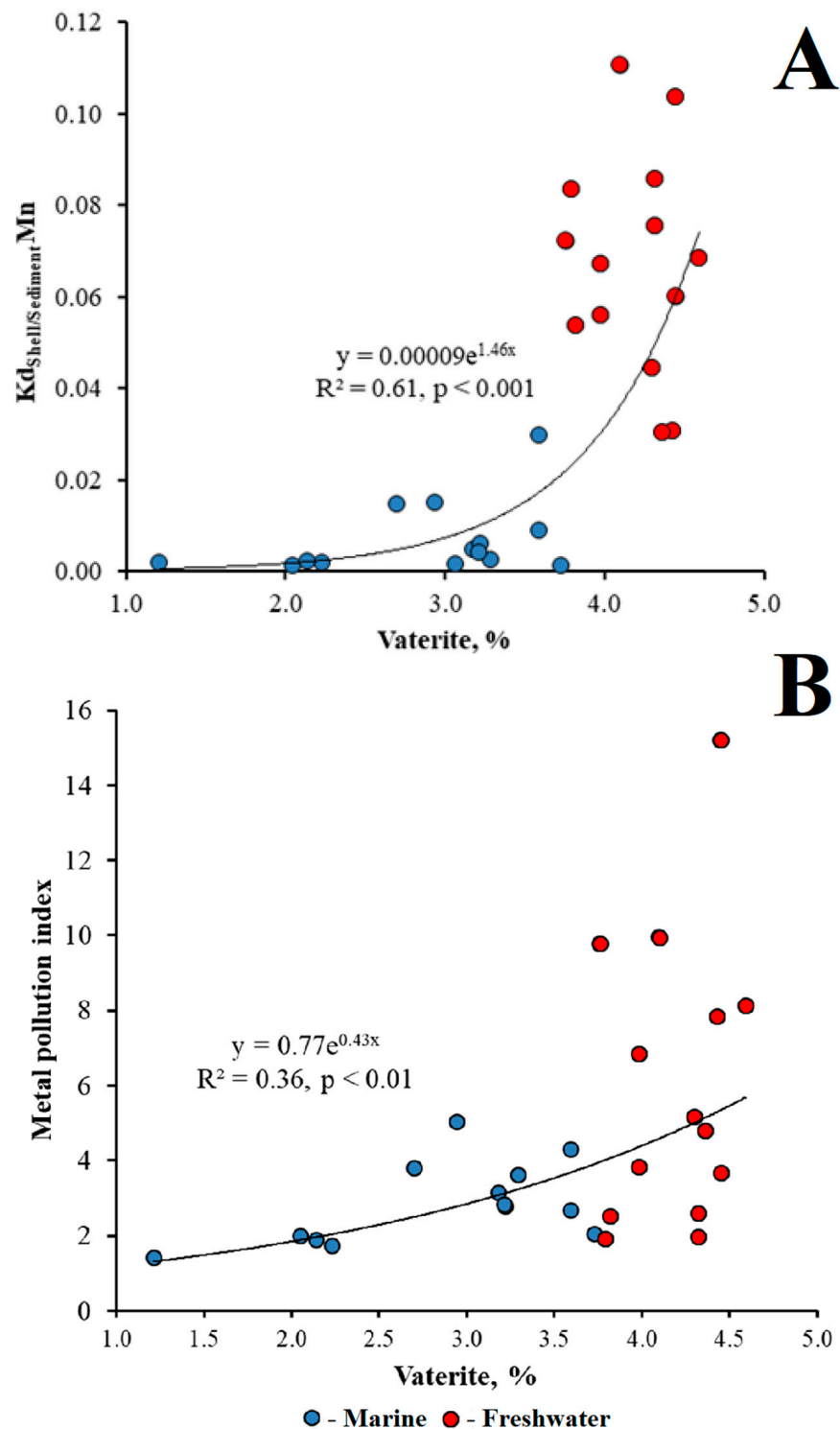


Figure 7. (A)—regression relationship between percentage of vaterite in mussels' shells and distribution coefficient between shell and sediment; (B)—regression relationship between percentage of vaterite in mussels' shells and values of metal pollution index.

It is worth noting that there was an increase in the MPI value with an increase in vaterite percentage of the shells ($R^2 = 0.34, p < 0.01$) when both marine and freshwater species were considered (Figure 7B), although this relationship does not necessarily reflect the causality because the freshwater mussels exhibit generally higher vaterite proportion and trace metal concentrations in the shells.

4. Discussion

4.1. Differences in Element Concentrations between Marine and Freshwater Mussels

The bivalve mussels' shells (*Unio* sp.) are a suitable environmental archive in aquatic ecosystems for a period of several years (i.e., [36]). Both marine and freshwater shells from the White Sea basin have a lifespan of four to five years. Similarly, Far Eastern mussels' species, including freshwater *B. beringiana* and marine *Mytilus trossulus*, can provide environmental information for the last 5–6 years. Generally, freshwater shells are known to exhibit more significant variation in the chemical composition compared to that of marine species (i.e., [6]). Results of the present study on localities' and species' identity control also indicate on more diversified chemical composition of shells and habitats in freshwater environments compared to marine biotopes. A comparison of trace element concentrations in marine and freshwater mussels' shells shows that the marine shells contain 1.5 to 9.4 times more Sr, S, Mg, Na, Li, and Zn. A first possible explanation is due to mineralogical control on element accumulation in shells, as follows from the difference in element compatibility to crystalline lattice of aragonite versus calcite [37]. In the present study, we found that calcite may constitute up to 67% of shells of marine mussels *Mytilus* (Table 2). The above listed elements are known to be highly mobile in aquatic ecosystems, including the Severnaya Dvina River Basin [38]. In addition to mineralogical control, another governing factor of element accumulation in shells is the type of sediments as confirmed by a relationship between Sr and S concentrations in freshwater mussels [33]. The elemental composition of the marine mussels' shells did not exhibit such a relationship with sediment of marine biotopes, because the latter are usually more homogeneous than freshwater ones, and marine mussels have significant variability of suitable biotope depth. Besides, the sediment was dominated by gravel and sand with scarce aquatic vegetation in biotopes where the studied species of the marine mussels were collected [24].

Quantitative assessment of metal concentration in mussels' shells demonstrated that freshwater bivalves' shells contain greater concentration of several elements, including Al, Ba, Ti, Fe, Mn, K, and Cu. These metals are likely to be controlled by sediment composition (clays, Fe hydroxides, and organic matter) in boreal and subarctic biotopes [33]. The MPI exhibited significant differences between marine and freshwater samples ($p < 0.05$), and it also differed between studied mussels' species ($p < 0.005$). The highest total concentration of metals was found in freshwater mussels' species *Anodonta anatina* and *Unio* sp. from the Onega River basin and from the Severnaya Dvina River basin. *Beringiana beringiana* from the Khalaktyrka River basin, *Mytilus trossulus* from the Avacha Bay, and *Mytilus edulis* from the White Sea basin had lower values of the MPI.

Mussels from freshwater basin of the Kamchatka Peninsula and from the Avacha Bay contain the lowest concentration of metals, and the highest values of one is determined for mussels' shells from basins of Northwestern Russia. It is, therefore, possible that high concentrations of colloidal Fe and DOM in NW subarctic settings, well-established in the Severnaya Dvina basin, including its estuarine zone [39,40], and lack of colloidal metals in DOM-poor rivers of the Kamchatka Peninsula [41] explain the drastic differences in metal accumulation in shells of mussels inhabiting these two regions.

The features of some less mobile metals (Al, Mn, Fe, and Ba) accumulation in freshwater mussels are known to be dependent on the habitat's environment [3,7,33,42]. In this study, we identified a number of trace elements (K, Al, Mn, Fe, light REE, Pb, Zr, Cu, Ba, and Ti) that exhibited sizably (a factor of 2.6 to 10) higher concentrations in freshwater compared to marine mussels' shells. It is envisaged that this reflects a habitat-controlled element uptake by freshwater shells. Indeed, the highest concentrations of these elements were found in the eurybiontic species, such as *A. anatina*, which inhabits silt-rich parts of the river bottom with generally higher concentration of trace metals in the substrate compared to sand and gravel bottom habitats. These trace elements can be taken up by mollusks from adsorbed/exchangeable complex on the surface of clays or river suspended matter (K, Pb, Cu, Ba, and Mn), or in the form of organic and organo-mineral colloids

(Al, Fe, LREE, Pb, Zr, Cu, and Ti) as follows from geochemical analysis of riverine particulate and colloidal elemental composition [39,43,44].

4.2. Relationships between Mineralogical and Chemical Composition of Bivalve Shells

Piwoni-Piórewicz et al. [45] reported that correct assessment of seawater environments using *Mytilus* shells depends on age of studied mussels, because the percentage of aragonite positively correlates with shell's size and negatively correlates with concentrations of several metals (Na, Cd, Cu, U, V, Zn, and Pb). Our results support a negative relationships between concentration of Na and Zn, and aragonite percentage in shells, although weak positive correlations were observed between Cu and Pb concentration and the aragonite and vaterite proportion. The presence of vaterite in freshwater bivalves can mark a disrupted biomineralization process [46] and it leads to enhanced accumulation of Mg and Ba, as well as organic matter, compared to aragonite shells [47]. Such a positive relationship between organic matter's level and vaterite presence in bivalve shells is consistent with a correlation between vaterite percentage and Mn:Ca ratio ($R_{\text{Spearman}} = 0.76$, $p < 0.01$). The latter is reported to be an indicator of eutrophication in water bodies [7]. It is interesting that positive correlations ($p < 0.01$) were also observed between vaterite percentage and Ca-normalized concentrations of other trace metals, which are known to be linked to organic complexes or colloids, especially in freshwater habitats (Al, Cu, Fe, Ti, Zr, and REE). The latter is demonstrated by size-fractionation procedure of colloid characterization in the Severnaya Dvina River [39].

The vaterite content in shells correlated with $K_d \text{ Shell/Sediment}$ of Mn (Figure 7A). The percentage of vaterite in shell is known to correlate with OM level in certain localities of the water body [47]. Given that the level of organic matter in the studied freshwater localities is higher compared to marine ones (Mann–Whitney criterion, $p < 0.001$), and that OM can bind a number of trace metals in strong, potentially bioavailable complexes, the mineralogical control on elementary composition of shells via vaterite presence is not straightforward and requires further investigation.

Generally, incorporations of ions into CaCO_3 structure exhibits strong crystallographic control, i.e., aragonite allows easier substitution of Ca^{2+} ion to Sr^{2+} , Ba^{2+} , and Na^+ ions compared to calcite [48–50], whereas the latter preferentially incorporates Mg^{2+} ion [51,52]. Further, the total content of Ca in aragonite shells is usually lower than that in calcite shells [53]. In accordance with these principles, we found a lower value of Sr:Ca ratio ($0.51 \pm 0.23 \text{ mmol/mol}$, $n = 14$) in aragonite shells compared to that in calcite shells ($1.55 \pm 0.19 \text{ mmol/mol}$, $n = 15$) (Mann–Whitney U test, $p < 0.001$). It has been shown for freshwater aragonite shells of Unionidae mussels *Lampsilis cardium* and *Hyriopsis* sp. [11] that Sr:Ca ratio in shells may be related to Sr concentration in water during vegetative (summer) period [21]. The present study does not support this observation for marine and freshwater bivalves ($p < 0.05$), because they did not differ by Sr distribution coefficients between shell and water ($p > 0.05$). A possible reason of significant differences in Sr $K_d \text{ Shell/Sediment}$ values between marine and freshwater bivalves could be the local environment in a certain bottom biotope, such as sediment chemical and mineralogical composition. Overall, the observed differences in $K_d \text{ Shell/Water}$ between marine and freshwater samples may be related to more homogenous bottom environment in marine biotopes in contrast to more heterogeneous environments in freshwater biotopes.

4.3. Elemental Ratios in Shells (Alkalis, Alkaline-Earth Metals, and Divalent Heavy Metals)

The biological control of Na accumulation was revealed based on Ca-normalized concentrations ($R^2 = 0.301$, $p < 0.05$) because $K_d \text{ Shell/Water}$ values of Na strongly correlated with the factor “species” ($R^2 = 0.937$, $p < 0.001$). In accordance with previous authors [54], there was a strong relationship between Na:Ca ratio in mussels' shells and water for both marine and freshwater samples ($R^2 = 0.815$, $p < 0.05$). This observation demonstrates clear environmental control on the Na concentration in the expial fluid, where Na incorporation

into CaCO_3 structure occurs across a very wide range (over four orders of magnitude) of Na concentration in the external milieu.

The Sr:Ca ratio demonstrated significant differences between marine and freshwater mussels (U Mann–Whitney criterion, $p < 0.00001$). We believe that it can be primarily linked to the presence of a high percentage of calcite in marine *Mytilus* shells, whereas all freshwater mussels had aragonite composition. Moreover, the variance of Sr:Ca ratio among freshwater samples ($\text{CV} = 45.7\%$) was sizably higher than that among marine samples ($\text{CV} = 12.5\%$), which was consistent with the recent results of [6]. The Sr:Ca ratio exhibited strong dependence on sampling locality for both marine and freshwater habitats, as supported by the general linear model ($p < 0.001$). The $K_d^{\text{Shell/Water}}$ of Sr also demonstrated significant relationship with the geographical factor among both marine and freshwater samples ($R^2 = 0.616$, $p < 0.001$). Taken together, these observations support strong environmental control of Sr accumulation by studied samples of mussels.

Significant differences in Sr concentration were observed between *Anodonta* and *Beringiana* (Mann–Whitney criterion, $p < 0.01$) samples due to the specific lithology of the Severnaya Dvina River basin, having a sizable proportion of carbonate rocks. The latter are responsible for elevated Sr concentration in the river water [38] and, in turn, lead to Sr accumulation in freshwater mussels' shells [33]. In contrast, we did not observe significant differences between *Anodonta* and *Beringiana* samples by Ca-normalized concentration of Mg, which may be caused by the dominance of similar environmental niches for these two species. Similarly, there was no difference in the Ca-normalized Mg concentration between *Unio* and *Beringiana* samples.

Physiological control of Sr incorporation into shells of freshwater pearl mussel *Margaritifera margaritifera* was demonstrated by Bailey and Lear [16]. Other researchers noted biological control of Sr:Ca ratio in carbonate otoliths of marine species, in contrast to environmental control of freshwater ones (i.e., [20]), and results of this study also demonstrated environmental control on Sr accumulation by freshwater species.

The Mn:Ca is an important geochemical indicator, widely used for reconstruction of aquatic environments in marine and freshwater biotopes [5,6]. The Mn:Ca ratio values demonstrated a factor of six differences between studied mussels' species (H Kruskal–Wallis criterion, $p < 0.0001$), with the highest values found in freshwater mussels *Anodonta anatina* and *Beringiana beringiana* (Figure S5). These species inhabit biotopes with clay substrate; they borrow into sediments and, therefore, accumulate high Mn concentration from partially anoxic porewaters, where high concentrations of free Mn^{2+} ion occur [7]. Strong accumulation of Mn in bottom layers of the water column is fairly well-established across the boreal zone [55–58]. Other factors responsible for shell enrichment in Mn relative to Ca could be a bloom of Mn-accumulating phytoplankton [59,60], as it was demonstrated for shells of *Mytilus edulis* [61], *Isognomon ephippium* [62], and *Pleiodon spekkii* [63].

The lowest values of Mn:Ca ratio among freshwater samples were observed for mussels belonging to genus *Unio*. It may be explained by a sand-dominated type of substrate for *Unio* compared to *Anodonta* and *Beringiana* mussels; the latter usually inhabit biotopes with silt-rich bottom. The lowest Mn:Ca ratios among both marine and freshwater mussels were observed for genus *Mytilus*. It could be linked to specific attached lifestyle of *Mytilus* mussels, which prefer sand ground with abundant aquatic vegetation [24]. In contrast to clay-rich environments where other species inhabit, Mn porewater concentration in these sandy, macrophytes-dominated settings is quite low (i.e., [64]). Another interesting observation is that the greatest concentrations of Mn were observed for shells of *Beringiana*, and the lowest ones were observed for shells of marine mussels *Mytilus trossulus* (Figure S5). At the same time, Mn:Ca ratio was higher for *Mytilus edulis*, which inhabit biotopes with sandy and silted bottom, compared to *Mytilus trossulus*, collected from pebble substrate with aquatic vegetation. These results corroborate previous data, acquired in other biotopes of the European Subarctic [33].

Recently, Wang et al. [65] demonstrated that Sr:Ba ratio allows to distinguish marine and freshwater environments due to the differences in mobility of these elements. Our re-

sults support this observation because there are statistically significant differences between marine and freshwater samples by Sr:Ba ratio (Mann–Whitney criterion, $p < 0.001$). Univariate GLM evidenced strong relationship between individual site and Sr:Ba ratio, with additional influence of vaterite's percentage in shells as a covariate ($R^2 = 0.95$, $p < 0.001$). Moreover, there was an increase in Sr:Ba ratio in shells with a decrease of vaterite proportion ($R^2 = 0.64$, $p < 0.001$; Figure S6).

The pattern of Ba:Ca ratio was generally similar to the one of Mn:Ca ratio (Figure S7). However, the highest values of Ba:Ca ratio were found for freshwater species *Anodonta anatina* and *Unio pictorum*. *Beringiana beringiana* had lower values compared to the last two species (H Kruskal–Wallis criterion, $p < 0.0001$). The Ba:Ca ratio in marine mussels' shells was lower than that in freshwater ones in both western and eastern Eurasia basins studied in this work. Similar to Mn, the difference in Ba:Ca ratio between freshwater and marine mussels from these three regions may be explained by chemical composition of sediments (Table S3). Furthermore, the Ba:Ca ratio is directly related with primary productivity of water ecosystems; e.g., peaks of Ba:Ca ratio in shell profile of marine mussel *Donax gouldii* corresponded to increasing level of Chl *a* in the water column [6,66].

In marine settings, Ba has vertical distribution in the water column similar to that of nutrients [67]. Overall, regression relationships between Mn:Ca and Ba:Ca; and Pb:Ca and Ba:Ca (Figures S6 and S7) suggest that the primary productivity of water ecosystems, which is related to the type of bottom substrate, is among the factors controlling trace metal incorporation in the shells. The highest values of these elemental ratios correspond to soft bottom substrates like silt and clay, which usually exhibit higher primary productivity in the water column and macrophytes. For example, $K_d \text{ Shell/Sediment}$ is significantly different between studied mussels' species (H Kruskal–Wallis criterion, $p < 0.001$), with the highest values observed for *Beringiana beringiana* which inhabits silted bottom, and the lowest values recorded for mussels from the genus *Mytilus* originated from biotopes with a hard bottom substrate.

We found a positive relationship between Pb:Ca and Ba:Ca ratios in marine and freshwater samples ($R^2 = 0.60$, $p < 0.0001$; Figure S8). Increasing of Pb concentration in shells can be linked to increasing primary productivity of water ecosystems [63], as demonstrated for biotopes with silt sediments compared to sandy and pebble substrates. There are reports of positive correlations between Pb:Ca ratio and organic matter concentration in the sediment [68,69], because silt substrate led to high values of Pb concentration in shells of mussels' species compared to shells of mussels distributed on the sandy substrate [70]. Our study corroborates these former observations as it demonstrated significant relationships of Pb concentration in marine mussels' shells with the factor "locality" for marine mussels ($R^2 = 0.556$, $p < 0.005$).

4.4. Lithogenic Elements

Analysis of relationships between the locality factor and Al-normalized concentration of Sr and Ba in mussels' shells revealed patterns consistent with those observed by Wang et al. [65] for sediments. Al-normalized concentration helps to assess clay material passive incorporation into the shells. Normalization of trace element concentration to Al demonstrated that the lowest admixtures of clay materials and the lowest concentration of lithophilic elements are observed in marine mussels *Mytilus*. In contrast, freshwater mussels accumulated greater amount of lithophilic elements (Figure 3) and they differed significantly ($p < 0.05$) from marine mussels by Al-normalized concentration of Li, Na, Mg, p, S, K, Ca, Ti, Mn, Fe, Cu, Zn, Sr, Zr, Ba, REE, Pb, and U (Figure 4A). This can be explained by much higher suspended particulate matter (SPM) concentration in river water and lower Al concentration in marine SPM (which is served as food for filtrators) compared to riverine settings [71].

The Al-normalized data demonstrate that majority of metals were generally associated with silt-/clay-type materials, rich in organic matter, which were deposited in low-energy sedimentary environments [72,73]. Therefore, chemical and granulometric composition of

sediments essentially control the accumulation of trace metals in mussels' shells, specifically in freshwater localities with high variability of environmental conditions in bottom habitats.

There is only limited information on REE pattern in marine mussels' shells, which exhibited differences between several marine localities in the North Sea Basin [74]. We found that Pr and Nd concentrations in mussels' shells from the entire dataset (marine and freshwater samples) exhibit significant positive correlations with those of the sediment ($R_{\text{Spearman}} = 0.943$, $p < 0.01$ for Pr, and $R_{\text{Spearman}} = 0.886$, $p < 0.05$ for Nd). At the same time, the UCC-normalized concentrations of La, Ce, and Pr had no significant differences between marine and freshwater samples ($p > 0.01$), suggesting lack of environmental control, while such differences were significant for Nd and Gd ($p < 0.01$). We do not have a straightforward explanation for the contrasting behavior of light and middle REE. Tentatively, LREE are prone to form adsorbed complexes with mineral (clay) particles, and these complexes are similar for both marine and freshwater settings. In contrast, MREE are influenced by aqueous complexes with organic matter in river water and with inorganic ligands in marine environments and the bio-uptake of these complexes is different between different groups of mussels.

It is noteworthy that concentrations of La, Ce, Pr, Nd, and Gd normalized to their concentrations in sediments did not differ between marine and freshwater samples ($p > 0.05$). This suggests lack of physiological and mineralogical control on REE accumulation in shells. Presumably, these insoluble, biologically-indifferent elements enter the expallial fluid of the mussels in the form of suspended silicate particles. These particles are passively occluded (incorporated) into the CaCO_3 structure and essentially inherit the original chemical composition of the bottom substrate.

4.5. Element Distribution between Shells and Environment

The distribution coefficients of K and Na between shell and water were much higher for freshwater mussels compared to marine ones (Figure 5). It is primarily related to much higher concentrations of Na and K in seawater compared to the river water; this difference leads to decreased K_d values in shells of marine species. Thus, specific biological control of trace elements accumulation in marine mussels can be invoked. Similar mechanisms may operate for Mg and S (sulfate), although the difference in K_d of Mg and SO_4 between freshwater and seawater shells was not so important as for Na and K. Hence, active uptake or strong mineralogical control on the incorporation of these elements into calcite vs. aragonite have to be invoked. Indeed, we found positive correlations of Na and S concentrations to calcite percentage in mussels' shells, whereas lithophytic elements, such as Mn, Al, and Ba were correlated to aragonite and vaterite percentage, more abundant in shells from freshwater settings. Strontium was strongly controlled by percentage of calcite in shells, and the values of $K_d^{\text{Shell/Water}}$ for Sr (0.14–0.23) in *Mytilus* shells measured in this study were consistent with data reported for shells of marine bivalve *M. edulis* from the Hudson Bay (0.14–0.20) [75].

The PCA for $K_d^{\text{Shell/Water}}$ and $K_d^{\text{Shell/Sediments}}$ allowed to reveal the following features of elemental control. PC1 positively correlated to $K_d^{\text{Shell/Water}}$ of lithophilic elements in water, whereas PC2 was related to water chemistry near silt sediment, because this factor loadings were highest for Mn and S, that are known to accumulate at the bottom water layer–sediment interface. Although confidence intervals for marine and freshwater samples overlap, the standard deviation of freshwater mussels was much higher than that of marine ones, for both PC1 and PC2 variables (Figure S9). It is expected that this is an evidence of biological control during incorporation of trace elements in marine shell from surrounding water, and, respectively, the presence of environmental control of this process for freshwater mussels. It should be noted that the ensemble of marine and freshwater mussels represents three separate regions and water basins, including the freshwater basin and the related marine basin. According to the PCA results, marine and freshwater mussels exhibited similar patterns of accumulation of lithophilic elements (Li, Na, Mg, Al, and K) from surrounding water, whereas they differed by accumulation of Mn and S. Given that these

elements are typically enriched in the sediment–water interface, just in the habitat of bivalve mollusks, we conclude that marine mussels consume and accumulate fewer concentrations of Mn and S, due to living on habitats more open for water exchange and less stratified in these elements compared to freshwater ones.

The PCA results for Ca-normalized K_d Shell/Sediment values demonstrated that Factor 1 allowed to distinguish marine and freshwater samples (Mann–Whitney criterion, $p < 0.001$). This factor was related to the type of bottom substrate given its high positive loadings (0.7 to 0.9) for K_d Shell/Sediments of Al, Mn, and lithophilic elements such as K, Ti, Fe, Zr, Ba, and REE. These elements were preferentially enriched in bottom sediments, compared to mussels' shells. Fe and Mn had strong correlation with Factor 1 (factor loadings were from 0.8 to 0.9). Factor 2 was related to concentrations of Na and Sr (0.975 and 0.622, respectively). K, Zr, and Ba exhibited moderate to low correlations with both Factors 1 and 2. Presumably, this group of elements was poorly related to the substrate chemical composition. At the same time, Factor 1 explained 44% of the total variance and factor 2 explained only 19% of the variance. Therefore, factor 1 was directly related to the bottom substrate in biotopes inhabited by studied mussels' species and it allowed distinguishing between marine and freshwater mollusk species according to their habitat preferences (Figure S9B). Factor 2 can be related to the water chemistry at the water–sediment interface, due to the presence of sulfur compounds in such settings (i.e., [33,76]).

Considering together the factors of both PCA treatments (K_d Shell/Water and K_d Shell/Sediment), we conclude that marine samples demonstrate lower variance for observed factors compared to freshwater samples. The exception is factor 2 for K_d Shell/Sediment samples, that were related to the water chemistry at the sediment interface, for both marine and freshwater samples. The concentration factor (F1) for K_d Shell/Water did not differ between marine and freshwater shells, although it had greater values of variance for freshwater samples. A number of labile elements had similar pattern in K_d Shell/Water of Li, Na, Mg, Al, and K for both freshwater and marine samples. Meanwhile, we found significant differences between marine and freshwater samples by factors related to the bottom substrate (factor 1 for K_d Shell/Sediment) and to the water layer (factor 2 for K_d Shell/Water). In fact, marine and freshwater mussels had different patterns of heavy metal (including Mn, Al, Fe, Ba, and Pb) accumulation, likely due to the presence of clays, OM, and sulfide—the main controlling factors—at the sediment surface and water–sediment interface in different degree in these settings. A number of other factors, such as the local environments of habitats together with metabolically driven mineralogical composition of shells, may also interfere in eventual control of major and trace element pattern in mussels' shells.

The hypothesis on the biological and environmental control of trace elements accumulation in mussels' shells was further confirmed via GLM treatment of the data on elemental composition of marine mussels *Mytilus*, which is represented as a separate group on the PCA plot. The lowest concentration of trace elements in their shells may be due to the fact that these mussels inhabit a saltwater environment with the highest water mineralization among all localities. Freshwater samples are distributed according to the total trace element content in shells (Figure S4A) and water mineralization in studied biotopes. Here, species could be ranged according to the MPI increase, from *Beringiana* to *Anodonta*, which reflects the influence of local environmental factors.

4.6. Biological and Environmental Control of Trace Element Accumulation in Mussels' Shells

Analysis of distribution coefficients between mussels' shells and water revealed a biological control on element accumulation, in particular, a factor 3, which acted on S, Li, and U. In studied settings, U is known to be redox-sensitive (e.g., [77]). Kriauciunas et al. [78] reconstructed variations of redox conditions in a Holocene marine coastal biotope based on the pattern of uranium concentrations in marine bivalve shells *Mytilus* from several layers of the outcrop. In the present study, species of marine mussels *Mytilus* from two remote regions (White Sea and Western Pacific) exhibited strong differences in accumulation of U from water, hence suggesting an environmental control. Pavlov

et al. [79] evidenced site-specific differences in concentrations of several elements (Sc, V, Cr, Fe, Zn, Rb, Ta, REE (La, Ce, Sm, Eu)) in marine mussels' shells. At the same time, As, Se, Rb, and Ba did not demonstrate such geographical features. In this study, we revealed differences in Ca-normalized concentrations of K, Fe, Al, Mn, Ba, Pb, Mg, La, Sr, S, Na, and La in shells among observed localities (Kruskal–Wallis criterion, $p < 0.01$) (Table 3).

The PCA treatment revealed two factors which allow to distinguish marine and freshwater mussels (Figure S11A). Factor 1 showed the difference in trace elements concentrations between marine mussels *Mytilus trossulus* originating from the Kamchatka Peninsula, and *Mytilus edulis* from basins of the Northeastern Europe (Mann–Whitney criterion, $p < 0.05$). Significant differences (Kruskal–Wallis criterion, $p < 0.005$) by Factor 2 were revealed not only between marine and freshwater samples but also among mussels' shells samples from each of the six studied localities. The median values of Factor 2 were generally higher for marine localities with relatively low variance compare to freshwater sites (Figure S10). It may be related to the mineralization of water in marine sites, given that F2 demonstrated greater values in marine shells due to its significant positive correlation with Na concentration.

Al-normalized element concentrations revealed greater variance for marine samples compared to freshwater ones (Figure S4B). A PCA graph showed that the ellipses of confidence intervals intersect. Significant differences between marine and freshwater samples were determined by F1, which had high loading for labile major cations and alkaline-earth metals (Li, Na, Mg, K, Ca, Sr, Ba), P, but also trace metals (Ti, Cu, Zn, Zr, Gd, Pb, and U). Presumably, these elements exhibit different pattern in marine and freshwater samples, reflecting both dissolved (labile elements) and sedimentary (P and trace metals) sources, including organic-matter-associated divalent trace metals. Factor 2 was related to Al-normalized concentrations of several REE, including La, Ce, and Nd, whereas factor 3 had the greatest positive correlations with Al-normalized concentrations of Fe, Mn, and Zr, hence reflecting elevated concentrations of these metals in several studied basins such as the Khalaktyrka River and the related Avacha Bay. The lowest values of this factor were determined for the Onega River basin that is located in the area of distribution of metamorphic rocks (granito-gneisses). These features of Fe and Mn distribution may be related to the presence of fine-grained sediments in specific localities. For example, we determined relatively high values of Al-normalized concentration of Fe and Mn in samples from Khalaktyrskoe Lake comparing to freshwater shells samples from the Onega River basin, which can be linked to sizable hydrothermal input of these metals in rivers of the Kamchatka Peninsula (i.e., [41]).

5. Conclusions

Elemental composition of marine and freshwater mussels' shells reflected the difference in the environment but also suggested a biological control on major and trace element accumulation in the marine environments. The biological control was less pronounced for freshwater mussels. The latter accumulated chemical elements in a wide range, depending on composition of the water column and sediments. A number of elements (K, REEs (La, Ce), and U) did not exhibit significant differences between marine and freshwater shells. Taken together, the elemental composition of 'external' compartments (i.e., water and sediment) together with 'internal' biological and mineralogical factors regulate concentrations of majority of trace elements in studied mussels' shells, as confirmed from the analysis of distribution coefficients between shells and environmental components.

Our results support negative relationships between concentrations of Na, Zn, and aragonite percentage in shells, although weak positive correlations were observed between Cu and Pb concentration and the aragonite and vaterite proportion. The vaterite content in shells correlated with K_d Shell/Sediment of Mn.

The Mn:Ca ratio values demonstrated the highest values among both marine and freshwater samples in freshwater mussels *Anodonta anatina* and *Beringiana beringiana*, and the lowest Mn:Ca ratios were observed for genus *Mytilus*.

Calcium-normalized distribution coefficients of elements K_d between shell and environment were also distinctly different between marine and freshwater mussels. The K_d $_{Shell/Water}$ values of Li, Mg, Mn ($p < 0.01$), and U ($p < 0.05$) were significantly different between marine species, whereas the K_d $_{Shell/Water}$ values of Li, Na, S, K, and Mn were significantly different for freshwater mussels from distinct geographical regions ($p < 0.01$). Multiparametric statistics revealed that all marine mussels accumulated trace elements under influence of two factors.

Further studies are needed to apply the developed approaches for other taxa of marine and freshwater mollusks. The spatial heterogeneity of trace metal distribution within the shells should also help to constrain specific seasonal events and characterize inter-annual variations, needed for better understanding of controlling mechanisms.

Supplementary Materials: The following supporting information can be downloaded at: <https://www.mdpi.com/article/10.3390/w15203625/s1>. Figure S1: Upper crust-normalized REE pattern of the average values in the bivalve mollusks' shells; Figure S2: Bottom sediment-normalized REE pattern of the average values in the bivalve mollusks' shells; Figure S3: Mean ratio of trace elements concentrations in marine to fresh water localities. Error bars indicate s.e.m.; Figure S4: A—Mean values of the metal (Li, Na, Mg, Al, P, K, Ti, Mn, Fe, Cu, Zn, Sr, Zr, Ba, La, Ce, Pr, Nd, Gd, Pb, and U) pollution index for studied samples of marine ($n = 4-5$) and freshwater mussels ($n = 4-6$). Significant differences are shown by letters (a—no significant differences ($p > 0.05$), b—differences are significant at $p < 0.05$); B—Mean values of the metal (Li, Na, Mg, Al, P, K, Ti, Mn, Fe, Cu, Zn, Sr, Zr, Ba, La, Ce, Pr, Nd, Gd, Pb, and U) pollution index for studied species of marine ($n = 5-9$) and freshwater mussels ($n = 5$); Figure S5: Comparison of Mn:Ca-ratio (mmol/mol) in shells of studied species of bivalve mollusks ($n = 5$ to 9). The differences between Mn:Ca-ratio values among samples are significant at $p < 0.00001$. Error bars indicate s.e.m.; Figure S6: Regression relationship between Sr:Ba-ratio in freshwater (red circles) and marine (blue circles) mussels' shells and percentage of vaterite; Figure S7: Regression relationships between Ba:Ca-ratio and Mn:Ca-ratio in bivalve shells samples. Blue circles, marine mussels ($N = 15$); hatched circles, freshwater mussels ($N = 14$); Figure S8: The power relationships between Ba:Ca-ratio and Pb:Ca-ratio in bivalve shells samples. Yellow labels show samples from biotopes with silt sediment and red labels show samples from biotopes with dominant sandy deposits; Figure S9: A—PCA factorial graph $F1 \times F2$ for K_d $_{Shell/Water}$. The samples are shown by markers: blue ones present marine samples; red ones present freshwater samples. Ellipses indicate 95% confidence interval. B—PCA factorial graph $F1 \times F2$ for K_d $_{Shell/Sediment}$. The samples are shown by markers: blue ones present marine samples; red ones present freshwater samples. Ellipses indicate 95% confidence interval; Figure S10: Median values of Factor 2 for studied samples of mussels from marine (blue columns) and freshwater (red columns) localities; Figure S11: A—Normed PCA factorial graph $F1 \times F2$ of marine (blue circles) and freshwater (red circles) samples. Ellipses indicate 95% confidence interval; B—PCA factorial graph $F1 \times F3$ of Al-normalized concentration of trace elements in freshwater and marine samples. The samples are shown by markers: blue ones present marine samples; red ones present freshwater samples. Ellipses indicate 95 % confidence interval; Table S1: Elemental composition of freshwater bivalve shells (ppm, dry weight); Table S2: Elemental composition of marine bivalve shells (ppm, dry weight); Table S3: Elemental composition water and bottom sediments; Table S4: Ca-normalized distribution coefficients between mussels' shells and water; Table S5: Comparison of normalized concentration of Na, Mn, Ba, Mg, and Sr in marine and freshwater environments (✓— $p < 0.01$, ✓*— $p < 0.05$, ×— $p > 0.05$); Table S6: Correlations between Ca-normalized concentrations of Li, Na, S and U in mussels' shells, water, and sediment ($n = 6$). Significant correlations are marked by an asterisk. Table S7: Relationships of Ca-normalized trace element concentrations in mussels' shells with "species" factor, determined using GLM (relationships are significant at $p < 0.05$, marked by an asterisk). Table S8: Relationships of Ca-normalized trace element concentrations in mussels' shells with "locality" factor, determined using GLM (relationships are significant at $p < 0.01$). Statistically significant relationships are marked by an asterisk. Table S9: GLM for Al-normalized concentration of trace elements in freshwater mussels' shells, Factor: Locality (relationships are significant at $p < 0.01$). Table S10: GLM for Al-normalized concentration of trace elements in marine mussels' shells, Factor: Locality (relationships are significant at $p < 0.01$). Table S11: Relationships of distribution coefficients (K_d $_{Shell/Water}$) of elements between mussels' shells and water with factor "locality" determined using

GLM (relationships are significant at $p < 0.01$). Table S12: Relationships of element distribution coefficients (K_d Shell/Water) with species factor determined using GLM (relationships are significant at $p < 0.01$). Table S13: Spearman correlation coefficients between content of calcite, aragonite, vaterite and Ca-normalized element concentrations in bivalve shells. One asterisk indicates a significant correlation at $p < 0.05$, two asterisks indicate a significant correlation at $p < 0.01$. A dash indicates no statistically significant correlation. Table S14: Spearman correlation coefficients between content of calcite, aragonite, vaterite and Al-normalized element concentrations. One asterisk indicates a significant correlation at $p < 0.05$, two asterisks indicate a significant correlation at $p < 0.01$. A dash indicates no statistically significant correlation.

Author Contributions: Methodology, A.A.L., G.V.B., T.A.E., I.S.K., A.V.K., A.V.M., V.M. and O.S.P.; Investigation, A.A.L., I.A.K., G.V.B., T.A.E., M.Y.G., I.S.K., A.V.K., A.V.M., V.M., A.R.S., A.A.S. and O.S.P.; Writing—original draft, A.A.L., I.A.K. and O.S.P.; Writing—review & editing, A.A.L., O.S.P. and I.N.B. All authors have read and agreed to the published version of the manuscript.

Funding: This research was funded by the Russian Science Foundation, Grant Number 21-17-00126 (including shells' sampling, species determination, molecular analyses, and analysis of the trace element composition of shells, water, and bottom sediment samples). X-ray diffraction analysis was carried out using the equipment of the Core Facility Center 'Arktika' of Northern (Arctic) Federal University (project RFMEFI59419X0016). OP is grateful to the partial support from the ANR MeLiCa and TSU program "Priority 2030".

Data Availability Statement: Not available.

Conflicts of Interest: The authors declare no conflict of interest.

References

- Schöne, B.R. *Arctica islandica* (Bivalvia): A unique paleoenvironmental archive of the northern North Atlantic Ocean. *Glob. Planet. Chang.* **2013**, *111*, 199–225. [\[CrossRef\]](#)
- Schöne, B.R.; Page, N.A.; Rodland, D.L.; Fiebig, J.; Baier, S.; Helama, S.O.; Oschmann, W. ENSO-coupled precipitation records (1959–2004) based on shells of freshwater bivalve mollusks (*Margaritifera falcata*) from British Columbia. *Int. J. Earth Sci.* **2007**, *96*, 525–540. [\[CrossRef\]](#)
- Bolotov, I.N.; Pokrovsky, O.S.; Auda, Y.; Bepalaya, J.V.; Vikhrev, I.V.; Gofarov, M.Y.; Lyubas, A.A.; Viers, J.; Zouiten, C. Trace element composition of freshwater pearl mussels *Margaritifera* spp. across Eurasia: Testing the effect of species and geographic location. *Chem. Geol.* **2015**, *402*, 125–139. [\[CrossRef\]](#)
- Watanabe, T.; Suzuki, M.; Komoto, Y.; Shirai, K.; Yamazaki, A. Daily and annual shell growth in a long-lived freshwater bivalve as a proxy for winter snowpack. *Palaeogeogr. Palaeoclimatol. Palaeoecol.* **2021**, *569*, 110346. [\[CrossRef\]](#)
- Sklyarov, E.V. *Interpretation of Geochemical Data*; Internet Inzhiniring: Moscow, Russia, 2001; p. 288. (In Russian)
- Peharda, M.; Schöne, B.R.; Black, B.A.; Corrège, T. Advances of sclerochronology research in the last decade. *Palaeogeogr. Palaeoclimatol. Palaeoecol.* **2021**, *570*, 110371. [\[CrossRef\]](#)
- Zhao, L.; Walliser, E.O.; Mertz-Kraus, R.; Schöne, B.R. Unionid shells (*Hyriopsis cumingii*) record manganese cycling at the sediment–water interface in a shallow eutrophic lake in China (Lake Taihu). *Palaeogeogr. Palaeoclimatol. Palaeoecol.* **2017**, *484*, 97–108. [\[CrossRef\]](#)
- Gillikin, D.P.; Lorrain, A.; Navez, J.; Taylor, J.W.; André, L.; Keppens, E.; Baeyens, W.; Dehairs, F. Strong biological controls on Sr/Ca ratios in aragonitic marine bivalve shells. *Geochem. Geophys. Geosystems* **2005**, *6*, 1–15. [\[CrossRef\]](#)
- Carré, M.; Bentaleb, I.; Bruguier, O.; Ordinola, E.; Barrett, N.T.; Fontugne, M. Calcification rate influence on trace element concentrations in aragonitic bivalve shells: Evidences and mechanisms. *Geochim. Et Cosmochim. Acta* **2006**, *70*, 4906–4920. [\[CrossRef\]](#)
- Chamberlayne, B.K.; Tyler, J.J.; Gillanders, B.M. Elemental concentrations of waters and bivalves in the fresh to hypersaline Coorong Lagoons, South Australia: Implications for palaeoenvironmental studies. *Estuar. Coast. Shelf Sci.* **2021**, *255*, 107354. [\[CrossRef\]](#)
- Geeza, T.J.; Gillikin, D.P.; Goodwin, D.H.; Evans, S.D.; Watters, T.; Warner, N.R. Controls on magnesium, manganese, strontium, and barium concentrations recorded in freshwater mussel shells from Ohio. *Chem. Geol.* **2019**, *526*, 142–152. [\[CrossRef\]](#)
- Schleinkofer, N.; Raddatz, J.; Evans, D.; Gerdes, A.; Flögel, S.; Voigt, S.; Büscher, J.V.; Wisshak, M. Compositional variability of Mg/Ca, Sr/Ca, and Na/Ca in the deep-sea bivalve *Acesta excavata* (Fabricius, 1779). *PLoS ONE* **2021**, *16*, e0245605. [\[CrossRef\]](#) [\[PubMed\]](#)
- Zhao, L.; Schöne, B.R.; Mertz-Kraus, R. Controls on strontium and barium incorporation into freshwater bivalve shells (*Corbicula fluminea*). *Palaeogeogr. Palaeoclimatol. Palaeoecol.* **2017**, *465*, 386–394. [\[CrossRef\]](#)
- Marali, S.; Schöne, B.R.; Mertz-Kraus, R.; Griffin, S.M.; Wanamaker, A.D.; Matras, U.; Butler, P.G. Ba/Ca ratios in shells of *Arctica islandica*—potential environmental proxy and crossdating tool. *Palaeogeogr. Palaeoclimatol. Palaeoecol.* **2017**, *465*, 347–361. [\[CrossRef\]](#)

15. Takesue, R.K.; Bacon, C.R.; Thompson, J.K. Influences of organic matter and calcification rate on trace elements in aragonitic estuarine bivalve shells. *Geochim. Et Cosmochim. Acta* **2008**, *72*, 5431–5445. [\[CrossRef\]](#)
16. Bailey, T.R.; Lear, C.H. Testing the effect of carbonate saturation on the Sr/Ca of biogenic aragonite: A case study from the River Ehen, Cumbria, UK. *Geochem. Geophys. Geosystems* **2006**, *7*, Q03019. [\[CrossRef\]](#)
17. Lorrain, A.; Gillikin, D.P.; Paulet, Y.-M.; Chauvaud, L.; Mercier, A.L.; Navez, J.; André, L. Strong kinetic effects on Sr/Ca ratios in the calcitic bivalve *Pecten maximus*. *Geology* **2005**, *33*, 965–968. [\[CrossRef\]](#)
18. Lazareth, C.E.; Le Cornec, F.; Candaudap, F.; Freyrier, R. Trace element heterogeneity along isochronous growth layers in bivalve shell: Consequences for environmental reconstruction. *Palaeogeogr. Palaeoclimatol. Palaeoecol.* **2013**, *373*, 39–49. [\[CrossRef\]](#)
19. Freitas, P.S.; Clarke, L.J.; Kennedy, H.; Richardson, C.A.; Abrantes, F. Environmental and biological controls on elemental (Mg/Ca, Sr/Ca and Mn/Ca) ratios in shells of the king scallop *Pecten Maximus*. *Geochim. Et Cosmochim. Acta* **2006**, *70*, 5119–5133. [\[CrossRef\]](#)
20. Brown, R.J.; Severin, K.P. Otolith chemistry analyses indicate that water Sr:Ca is the primary factor influencing otolith Sr: Ca for freshwater and diadromous fish but not for marine fish. *Can. J. Fish. Aquat. Sci.* **2009**, *66*, 1790–1808. [\[CrossRef\]](#)
21. Izumida, H.; Yoshimura, T.; Suzuki, A.; Nakashima, R.; Ishimura, T.; Yasuhara, M.; Inamura, A.; Shikazono, N.; Kawahata, H. Biological and water chemistry controls on Sr/Ca, Ba/Ca, Mg/Ca and $\delta^{18}\text{O}$ profiles in freshwater pearl mussel *Hyriopsis* sp. *Palaeogeogr. Palaeoclimatol. Palaeoecol.* **2011**, *309*, 298–308. [\[CrossRef\]](#)
22. Fröhlich, L.; Siebert, V.; Huang, Q.; Thébault, J.; Jochum, K.P.; Schöne, B.R. Deciphering the potential of Ba/Ca, Mo/Ca and Li/Ca profiles in the bivalve shell *Pecten maximus* as proxies for the reconstruction of phytoplankton dynamics. *Ecol. Indic.* **2022**, *141*, 109121. [\[CrossRef\]](#)
23. Freitas, P.S.; Clarke, L.J.; Kennedy, H.; Richardson, C.A. Manganese in the shell of the bivalve *Mytilus edulis*: Seawater Mn or physiological control? *Geochim. Et Cosmochim. Acta* **2016**, *194*, 266–278. [\[CrossRef\]](#)
24. Naumov, A.D. *Bivalves of the White Sea. Experience of Ecologic-Faunistic Analysis*; ZIN, Russian Academy of Sciences: St. Petersburg, Russia, 2006; p. 499. (In Russian)
25. Bolotov, I.N.; Kondakov, A.V.; Konopleva, E.S.; Vikhrev, I.V.; Aksenova, O.V.; Aksenov, A.S.; Bepalaya, Y.V.; Borovskoy, A.V.; Danilov, P.P.; Dvoryankin, G.A.; et al. Integrative taxonomy, biogeography and conservation of freshwater mussels (Unionidae) in Russia. *Sci. Rep.* **2020**, *10*, 3072. [\[CrossRef\]](#)
26. Konopleva, E.S.; Bolotov, I.N.; Vikhrev, I.V.; Gofarov, M.Y.; Kondakov, A.V. An integrative approach underscores the taxonomic status of *Lamellidens exolegens*, a freshwater mussel from the Oriental tropics (Bivalvia: Unionidae). *Syst. Biodivers.* **2017**, *15*, 204–217. [\[CrossRef\]](#)
27. Konopleva, E.S.; Pfeiffer, J.M.; Vikhrev, I.V.; Kondakov, A.V.; Gofarov, M.Y.; Aksenova, O.V.; Lunn, Z.; Chan, N.; Bolotov, I.N. A new genus and two new species of freshwater mussels (Unionidae) from western Indochina. *Sci. Rep.* **2019**, *9*, 4106. [\[CrossRef\]](#) [\[PubMed\]](#)
28. Bolotov, I.N.; Makhrov, A.A.; Gofarov, M.Y.; Aksenova, O.V.; Aspholm, P.E.; Bepalaya, Y.V.; Kabakov, M.B.; Kolosova, Y.S.; Kondakov, A.V.; Ofenböck, T.; et al. Climate Warming as a Possible Trigger of Keystone Mussel Population Decline in Oligotrophic Rivers at the Continental Scale. *Sci. Rep.* **2018**, *8*, 35. [\[CrossRef\]](#)
29. Tomilova, A.A.; Lyubas, A.A.; Kondakov, A.V.; Vikhrev, I.V.; Gofarov, M.Y.; Kolosova, Y.S.; Vinarski, M.V.; Palatov, D.M.; Bolotov, I.N. Evidence for Plio-Pleistocene Duck Mussel Refugia in the Azov Sea River Basins. *Diversity* **2020**, *12*, 118. [\[CrossRef\]](#)
30. Folmer, O.; Black, M.; Hoeh, W.; Lutz, R.; Vrijenhoek, R. DNA primers for amplification of mitochondrial cytochrome c oxidase subunit I from diverse metazoan invertebrates. *Mol. Mar. Biol. Biotechnol.* **1994**, *3*, 294–299.
31. Hall, T.A. BioEdit: A user-friendly biological sequence alignment editor and analysis program for Windows 95/98/NT. *Nucleic Acids Symp. Ser.* **1999**, *41*, 95–98.
32. Johnson, M.; Zaretskaya, I.; Raytselis, Y.; Merezhuik, Y.; McGinnis, S.; Madden, T.L. NCBI BLAST: A better web interface. *Nucleic Acids Res.* **2008**, *36*, W5–W9. [\[CrossRef\]](#)
33. Lyubas, A.A.; Tomilova, A.A.; Chupakov, A.V.; Vikhrev, I.V.; Travina, O.V.; Orlov, A.S.; Zubrii, N.A.; Kondakov, A.V.; Bolotov, I.N.; Pokrovsky, O.S. Iron, Phosphorus and Trace Elements in Mussels' Shells, Water, and Bottom Sediments from the Severnaya Dvina and the Onega river basins (North western Russia). *Water* **2021**, *13*, 3227. [\[CrossRef\]](#)
34. Usero, J.; Gonzalez-Regalado, E.; Gracia, I. Trace metals in the bivalve molluscs *Ruditapes decussatus* and *Ruditapes philippinarum* from the Atlantic coast of southern Spain. *Environ. Int.* **1997**, *23*, 291–298. [\[CrossRef\]](#)
35. Sedeño-Díaz, J.E.; López-López, E.; Mendoza-Martínez, E.; Rodríguez-Romero, A.J.; Morales-García, S.S. Distribution coefficient and metal pollution index in water and sediments: Proposal of a new index for ecological risk assessment of metals. *Water* **2020**, *12*, 29. [\[CrossRef\]](#)
36. Ravera, O.; Cenci, R.; Beone, G.M.; Dantas, M.; Lodigiani, P. Trace element concentrations in freshwater mussels and macrophytes as related to those in their environment. *J. Limnol.* **2003**, *62*, 61–70. [\[CrossRef\]](#)
37. Markich, S.J.; Jeffree, R.A.; Burke, P.T. Freshwater bivalve shells as archival indicators of metal pollution from a copper-uranium mine in tropical Northern Australia. *Environ. Sci. Technol.* **2002**, *36*, 821–832. [\[CrossRef\]](#) [\[PubMed\]](#)
38. Chupakov, A.V.; Pokrovsky, O.S.; Moreva, O.Y.; Shirokova, L.S.; Neverova, N.V.; Chupakova, A.A.; Kotova, E.I.; Vorobyeva, T.Y. High resolution multi-annual riverine fluxes of organic carbon, nutrient and trace element from the largest European Arctic river, Severnaya Dvina. *Chem. Geol.* **2020**, *538*, 119491. [\[CrossRef\]](#)
39. Pokrovsky, O.S.; Viers, J.; Shirokova, L.S.; Shevchenko, V.P.; Filipov, A.S.; Dupré, B. Dissolved, suspended, and colloidal fluxes of organic carbon, major and trace elements in Severnaya Dvina River and its tributary. *Chem. Geol.* **2010**, *273*, 136–149. [\[CrossRef\]](#)

40. Pokrovsky, O.S.; Shirokova, L.S.; Viers, J.; Gordeev, V.V.; Shevchenko, V.P.; Chupakov, A.V.; Vorobieva, T.Y.; Candaudap, F.; Causserand, C.; Lanzanova, A.; et al. Fate of colloids during estuarine mixing in the Arctic. *Ocean Sci.* **2014**, *10*, 107–125. [\[CrossRef\]](#)
41. Dessert, C.; Gaillardet, J.; Dupre, B.; Schott, J.; Pokrovsky, O.S. Fluxes of high- versus low-temperature water-rock interactions in aerial volcanic areas: The example of the Kamchatka Peninsula, Russia. *Geochim. Cosmochim. Acta* **2009**, *73*, 148–169. [\[CrossRef\]](#)
42. Van Plantinga, A.A.; Grossman, E.L. Trace elements in mussel shells from the Brazos River, Texas: Environmental and biological control. *Biogeosciences Discuss.* **2019**, 1–27. [\[CrossRef\]](#)
43. Krickov, I.V.; Pokrovsky, O.S.; Manasypov, R.M.; Lim, A.G.; Shirokova, L.S.; Viers, J. Colloidal transport of carbon and metals by western Siberian rivers during different seasons across a permafrost gradient. *Geochim. Et Cosmochim. Acta* **2019**, *265*, 221–241. [\[CrossRef\]](#)
44. Krickov, I.V.; Lim, A.G.; Manasypov, R.M.; Loiko, S.V.; Vorobyev, S.N.; Shevchenko, V.P.; Dara, O.M.; Gordeev, V.V.; Pokrovsky, O.S. Major and trace elements in suspended matter of western Siberian rivers: First assessment across permafrost zones and landscape parameters of watersheds. *Geochim. Et Cosmochim. Acta* **2020**, *269*, 429–450. [\[CrossRef\]](#)
45. Piwoni-Piórewicz, A.; Kukliński, P.; Strekopytov, S.; Humphreys-Williams, E.; Najorka, J.; Iglowska, A. Size effect on the mineralogy and chemistry of *Mytilus trossulus* shells from the southern Baltic Sea: Implications for environmental monitoring. *Environ. Monit. Assess.* **2017**, *189*, 197. [\[CrossRef\]](#)
46. Spann, N.; Harper, E.M.; Aldridge, D.C. The unusual mineral vaterite in shells of the freshwater bivalve *Corbicula fluminea* from the UK. *Naturwissenschaften* **2010**, *97*, 743–751. [\[CrossRef\]](#) [\[PubMed\]](#)
47. Frenzel, M.; Harper, E.M. Micro-structure and chemical composition of vateritic deformities occurring in the bivalve *Corbicula fluminea* (Müller, 1774). *J. Struct. Biol.* **2011**, *174*, 321–332. [\[CrossRef\]](#) [\[PubMed\]](#)
48. Mavromatis, V.; Goetschl, K.E.; Grengg, C.; Konrad, F.; Purgstaller, B.; Dietzel, M. Barium partitioning in calcite and aragonite as a function of growth rate. *Geochim. Cosmochim. Acta* **2018**, *237*, 65–78. [\[CrossRef\]](#)
49. Föger, A.; Konrad, F.; Leis, A.; Dietzel, M.; Mavromatis, V. Effect of growth rate and pH on lithium incorporation in calcite. *Geochim. Cosmochim. Acta* **2019**, *248*, 14–24. [\[CrossRef\]](#)
50. Brazier, J.M.; Blanchard, M.; Meheut, M.; Schmitt, A.D.; Schott, J.; Mavromatis, V. Experimental and theoretical investigations of stable Sr isotope fractionation during its incorporation in aragonite. *Geochim. Cosmochim. Acta* **2023**, *358*, 134–147. [\[CrossRef\]](#)
51. Mavromatis, V.; Brazier, J.M.; Goetschl, K.E. Controls of temperature and mineral growth rate on Mg incorporation in aragonite. *Geochim. Cosmochim. Acta* **2022**, *317*, 53–64. [\[CrossRef\]](#)
52. Böttcher, M.E.; Dietzel, M. Metal-ion partitioning during low-temperature precipitation and dissolution of anhydrous carbonates and sulphates. *Eur. Mineral. Union Notes Mineral.* **2010**, *10*, 139–187. [\[CrossRef\]](#)
53. Iglowska, A.; Beldowski, J.; Chelchowski, M.; Chierici, M.; Kedra, M.; Przytarska, J.; Sowa, A.; Kukliński, P. Chemical composition of two mineralogically contrasting Arctic bivalves' shells and their relationships to environmental variables. *Mar. Pollut. Bull.* **2017**, *114*, 903–916. [\[CrossRef\]](#) [\[PubMed\]](#)
54. O'Neil, D.D.; Gillikin, D.P. Do freshwater mussel shells record road-salt pollution? *Sci. Rep.* **2014**, *4*, 7168. [\[CrossRef\]](#)
55. Pokrovsky, O.S.; Shirokova, L.S.; Zabelina, S.A.; Vorobieva, T.Y.; Moreva, O.Y.; Klimov, S.I.; Chupakov, A.V.; Shorina, N.V.; Kokryatskaya, N.M.; Audry, S.; et al. Size fractionation of trace elements in a seasonally stratified boreal lake: Control of organic matter and iron colloids. *Aquat. Geochem.* **2012**, *18*, 115–139. [\[CrossRef\]](#)
56. Pokrovsky, O.S.; Viers, J.; Dupré, B.; Chabaux, F.; Gaillardet, J.; Audry, S.; Prokushkin, A.S.; Shirokova, L.S.; Kirpotin, S.N.; Lapitsky, S.A.; et al. Biogeochemistry of carbon, major and trace elements in watersheds of northern Eurasia drained to the Arctic Ocean: The change of fluxes, sources and mechanisms under the climate warming prospective. *Comptes Rendus Geosci.* **2012**, *344*, 663–677. [\[CrossRef\]](#)
57. Pokrovsky, O.S.; Manasypov, R.M.; Chupakov, A.V.; Kopysov, S. Element transport in the Taz River, western Siberia. *Chem. Geol.* **2022**, *614*, 121180. [\[CrossRef\]](#)
58. Gordeev, V.V.; Kochenkova, A.I.; Starodymova, D.P.; Shevchenko, V.P.; Belorukov, S.K.; Lokhov, A.S.; Yakovlev, A.E.; Chernov, V.A.; Pokrovsky, O.S. Major and Trace Elements in Water and Suspended Matter of the Northern Dvina River and Their Annual Discharge into the White Sea. *Oceanology* **2021**, *61*, 994–1005. [\[CrossRef\]](#)
59. Kelemen, Z.; Gillikin, D.P.; Bouillon, S. Relationship between river water chemistry and shell chemistry of two tropical African freshwater bivalve species. *Chem. Geol.* **2019**, *526*, 130–141. [\[CrossRef\]](#)
60. Pokrovsky, O.S.; Shirokova, L.S. Diurnal variations of dissolved and colloidal organic carbon and trace metals in a boreal lake during summer bloom. *Water Res.* **2013**, *47*, 922–932. [\[CrossRef\]](#)
61. Vander Putten, E.; Dehairs, F.; Keppens, E.; Baeyens, W. High resolution distribution of trace elements in the calcite shell layer of modern *Mytilus edulis*: Environmental and biological controls. *Geochim. Et Cosmochim. Acta* **2000**, *64*, 997–1011. [\[CrossRef\]](#)
62. Lazareth, C.E.; Vander Putten, E.; André, L.; Dehairs, F. High-resolution trace element profiles in shells of the mangrove bivalve *Isognomon ehippium*: A record of environmental spatio-temporal variations? *Estuar. Coast. Shelf Sci.* **2003**, *57*, 1103–1114. [\[CrossRef\]](#)
63. Langlet, D.; Alleman, L.Y.; Plisnier, P.-D.; Hughes, H.; André, L. Manganese content records seasonal upwelling in Lake Tanganyika mussels. *Biogeosciences* **2007**, *4*, 195–203. [\[CrossRef\]](#)

64. Manasypov, R.M.; Pokrovsky, O.S.; Shirokova, L.S.; Auda, Y.; Zinner, N.S.; Kirpotin, S.N. Biogeochemistry of macrophytes, sediments and porewaters in lakes of permafrost peatlands, western Siberia. *Sci. Total Environ.* **2021**, *763*, 144201. [[CrossRef](#)] [[PubMed](#)]
65. Wang, A.; Wang, Z.; Liu, J.; Xu, N.; Li, H. The Sr/Ba ratio response to salinity in clastic sediments of the Yangtze River Delta. *Chem. Geol.* **2021**, *559*, 119923. [[CrossRef](#)]
66. Hatch, M.B.A.; Schellenberg, S.A.; Carter, M.L. Ba/Ca variations in the modern intertidal bean clam *Donax gouldii*: An upwelling proxy? *Palaeogeogr. Palaeoclimatol. Palaeoecol.* **2013**, *373*, 98–107. [[CrossRef](#)]
67. Komagoe, T.; Watanabe, T.; Shirai, K.; Yamazaki, A.; Uematu, M. Geochemical and microstructural signals in giant clam *Tridacna maxima* recorded typhoon events at Okinotori Island, Japan. *J. Geophys. Res. Biogeosci.* **2018**, *123*, 1460–1474. [[CrossRef](#)]
68. Church, T.M.; Bernat, M.; Sharma, P. Distribution of natural uranium, thorium, lead, and polonium radionuclides in tidal phases of a Delaware salt marsh. *Estuaries* **1986**, *9*, 2–8. [[CrossRef](#)]
69. Kim, G.; Alleman, L.Y.; Church, T.M. Accumulation records of radionuclides and trace metals in two contrasting Delaware salt marshes. *Mar. Chem.* **2004**, *87*, 87–96. [[CrossRef](#)]
70. Gillikin, D.P.; Dehairs, F.; Baeyens, W.; Navez, J.; Lorrain, A.; André, L. Inter- and intra-annual variations of Pb/Ca ratios in clam shells (*Mercenaria mercenaria*): A record of anthropogenic lead pollution? *Mar. Pollut. Bull.* **2005**, *50*, 1530–1540. [[CrossRef](#)]
71. Savenko, V.S. On the relationship between biogenic and terrigenous suspended particulate matter in the ocean. *Dokl. Acad. Sci.* **1999**, *364*, 251–254. Available online: https://scholar.google.com/scholar_lookup?title=On+the+relationship+between+biogenic+and+terrigenous+suspended+particulate+matter+in+the+ocean&author=Savenko,+V.S.&publication_year=1999&journal=Dokl.+Acad.+Sci.&volume=364&pages=251%E2%80%93254 (accessed on 23 July 2023).
72. Bubb, J.M.; Rudd, T.; Lester, J.N. Distribution of heavy metals in the River Yare and its associated broads III. Lead and zinc. *Sci. Total Environ.* **1991**, *102*, 189–208. [[CrossRef](#)]
73. Birch, G.F. An assessment of aluminum and iron in normalisation and enrichment procedures for environmental assessment of marine sediment. *Sci. Total Environ.* **2020**, *727*, 138123. [[CrossRef](#)] [[PubMed](#)]
74. Ponnurangam, A.; Bau, M.; Brenner, M.; Koschinsky, A. Mussel shells of *Mytilus edulis* as bioarchives of the distribution of rare earth elements and yttrium in seawater and the potential impact of pH and temperature on their partitioning behavior. *Biogeosciences* **2016**, *13*, 751–760. [[CrossRef](#)]
75. Faure, G.; Crocket, J.H.; Hueley, P.M. Some aspects of the geochemistry of strontium and calcium in the Hudson Bay and the Great Lakes. *Geochim. Et Cosmochim. Acta* **1967**, *31*, 451–461. [[CrossRef](#)]
76. Liu, C.; Shao, S.; Zhang, L.; Du, Y.; Chen, K.; Fan, C.; Yu, Y. Sulfur development in the water-sediment system of the algae accumulation embay area in Lake Taihu. *Water* **2019**, *11*, 1817. [[CrossRef](#)]
77. Vodyanitskii, Y.N. Chemical aspects of uranium behavior in soils: A review. *Eurasian Soil Sci.* **2011**, *44*, 862–873. [[CrossRef](#)]
78. Kriauciunas, V.V.; Iglovsky, S.A.; Lyubas, A.A.; Kuznetsova, I.A.; Kotova, E.I.; Shakhova, E.V.; Mironenko, K.A. New data on the paleogeography of the eastern coast of the Grönfjord Bay (western Spitsbergen Island) based on the study of Holocene deposits at Cape Finnisset using isotope-geochemical methods. *Bull. Tomsk Polytech. Univ. Eng. Georesources* **2020**, *331*, 171–183. [[CrossRef](#)]
79. Pavlov, D.F.; Bezuidenhout, J.; Frontasyeva, M.V.; Goryainova, Z.I. Differences in trace element content between non-indigenous farmed and invasive bivalve mollusks of the South African Coast. *Am. J. Anal. Chem.* **2015**, *6*, 886–897. [[CrossRef](#)]

Disclaimer/Publisher’s Note: The statements, opinions and data contained in all publications are solely those of the individual author(s) and contributor(s) and not of MDPI and/or the editor(s). MDPI and/or the editor(s) disclaim responsibility for any injury to people or property resulting from any ideas, methods, instructions or products referred to in the content.